

(20)

# A TRIDENT SCHOLAR PROJECT REPORT

NO. 192

"Applications Of Molecular Modeling To  
Transition State Energies And Conformations"

AD-A257 130



DTIC  
ELECTE  
NOV 12 1992  
S c D

UNITED STATES NAVAL ACADEMY  
ANNAPOLIS, MARYLAND

This document has been approved for public  
release and sale; its distribution is unlimited.

92-29340



**"Applications Of Molecular Modeling To  
Transition State Energies And Conformations"**

**A Trident Scholar Project Report**

by

**Midshipman John C. Mohs, Class of 1992**

**U.S. Naval Academy**

**Annapolis, Maryland**

Debra K. Heckendorn

**Adviser: Assistant Professor Debra K. Heckendorn  
Chemistry Department**

**DTIC QUALITY INSPECTED 4**

**Accepted for Trident Scholar Committee**

Francis J. Correll

**Chair**

8 May 1992

**Date**

Accession For	
NTIS GRA&I	<input checked="" type="checkbox"/>
DTIC TAB	<input type="checkbox"/>
Unannounced	<input type="checkbox"/>
Justification	
By	
Distribution/	
Availability Codes	
Dist	Avail and/or Special
A-1	

**USNA-1531-2**

REPORT DOCUMENTATION PAGE			Form Approved OMB No 0704-0188	
<small>Public reporting burden for this collection of information is estimated to average 1 hour per response, including the time for reviewing instructions, searching existing data sources, gathering and maintaining the data needed, and completing and reviewing the collection of information. Send comments regarding this burden estimate or any other aspect of this collection of information, including suggestions for reducing this burden, to Washington Headquarters Services, Directorate for Information Operations and Reports, 1215 Jefferson Davis Highway, Suite 1204, Arlington, VA 22202-4302, and to the Office of Management and Budget, Paperwork Reduction Project (0704-0188), Washington, DC 20503</small>				
1. AGENCY USE ONLY (Leave blank)	2. REPORT DATE 8 May 1992	3. REPORT TYPE AND DATES COVERED Final 1991/92		
4. TITLE AND SUBTITLE Applications of molecular modeling to transition state energies and conformations		5. FUNDING NUMBERS		
6. AUTHOR(S)  Mohs, John C.				
7. PERFORMING ORGANIZATION NAME(S) AND ADDRESS(ES)  U.S. Naval Academy, Annapolis, Md.		8. PERFORMING ORGANIZATION REPORT NUMBER  U.S.N.A. - TSPR; 192 (1992)		
9. SPONSORING/MONITORING AGENCY NAME(S) AND ADDRESS(ES)		10. SPONSORING/MONITORING AGENCY REPORT NUMBER		
11. SUPPLEMENTARY NOTES  Accepted by the U.S. Trident Scholar Committee				
12a. DISTRIBUTION/AVAILABILITY STATEMENT  This document has been approved for public release; its distribution is UNLIMITED.		12b. DISTRIBUTION CODE		
13. ABSTRACT (Maximum 200 words) A quantitative model of Baldwin's Rules for Ring Closure is constructed. Specific systems of interest are the lactonization and intramolecular Michael addition. A simulated transition state for each of these reactions is determined for simplified intermolecular systems. The intermolecular system for lactonization is the attack of water on protonated formic acid. The intermolecular system for the Michael addition is the attack of water on protonated acrylic acid. These transition state geometries are determined at the AM1 semi-empirical level. Results of these geometries are combined with force constants determined in this research to produce a molecular mechanics model for these transition states. Reactivity determinations made using this model for competitive lactonizations and intramolecular Michael additions are acceptable. A strain energy cutoff range for the Baldwin Rule 5-Endo-Trig has been determined to be between 63.9 and 80.4 kcal/mol.				
14. SUBJECT TERMS  chemistry - numerical solutions; organic compounds - synthesis; chemistry, organic; molecules		15. NUMBER OF PAGES 77		
		16. PRICE CODE		
17. SECURITY CLASSIFICATION OF REPORT UNCLASSIFIED	18. SECURITY CLASSIFICATION OF THIS PAGE UNCLASSIFIED	19. SECURITY CLASSIFICATION OF ABSTRACT UNCLASSIFIED	20. LIMITATION OF ABSTRACT	

### Abstract

A quantitative model of Baldwin's Rules for Ring Closure is constructed. Specific systems of interest are the lactonization and intramolecular Michael addition. A simulated transition state for each of these reactions is determined for simplified intermolecular systems. The intermolecular system for lactonization is the attack of water on protonated formic acid. The intermolecular system for the Michael addition is the attack of water on protonated acrylic acid. These transition state geometries are determined at the AM1 semi-empirical level. Results of these geometries are combined with force constants determined in this research to produce a molecular mechanics model for these transition states. Reactivity determinations made using this model for competitive lactonizations and intramolecular Michael additions are acceptable. A strain energy cutoff range for the Baldwin Rule 5-*Endo-Trig* has been determined to be between 63.9 and 80.4 kcal/mol.

Table of Contents

Abstract	1
Table of Contents	2
I. Introduction	3
II. Background: Computational Chemistry	5
IIA. Computational Chemistry: <i>Ab Initio</i> Methods	8
IIB. Computational Chemistry: Semi-Empirical Methods	15
IIC. Computational Chemistry: Molecular Mechanics	19
IID. Energy Minimization and Conformational Analysis	30
III. Transition State Theory and Activation Energy	36
IV. Approach	40
V. Experimental	41
VI. Integration of Parameters Into Force Field	55
VII. Conclusions and Further Research	72
Appendix A	73
References	75
Bibliography of Selected Readings	76

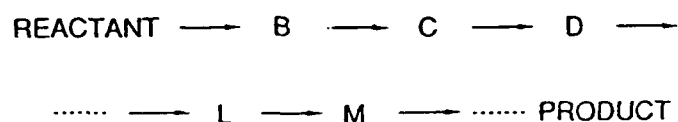
## I. Introduction.

This research is rooted in the fields of organic chemistry, physical chemistry, quantum mechanics, and classical physics. The results obtained in this research are especially applicable to the branch of chemistry known as synthetic organic chemistry, which concentrates on carbon-based chemical systems.

Synthetic organic chemists study a variety of reactions involving these carbon-based molecules. They study bonding within and between these molecules, and analyze chemical and physical properties of these systems. A synthetic organic chemist compiles this knowledge and concentrates on developing syntheses for new materials. Plastics, pharmaceuticals, fertilizers, insecticides, and food additives are a few examples of the types of compounds prepared by synthetic organic chemists.

Synthesis can be thought of as a plan, or strategy, for making a chemical compound. For instance, consider the generic synthesis in Scheme 1. This is a multi-step synthesis in which a reactant eventually is converted into the desired product. Say, for instance, that it is not known if step  $L \rightarrow M$  proceeds. There are two methods for determining if the step does indeed proceed. First, the synthetic chemist could perform the actual experiment. This requires a great deal of time and every precursor leading up to step  $L \rightarrow M$  must be synthesized if  $L$  is not commercially available, which is

usually the case. Second, the synthetic chemist could research the chemical literature for a similar reaction. However, this reaction will not have the exact reactivity as step  $L \rightarrow M$ , and the predictions based on this literature precedent may not work for the current system.



Scheme 1. Generic multi-step synthesis.

It would obviously be useful if the synthetic organic chemist had a set of guidelines which could be used in cases such as this. For the class of reaction investigated in this research, the ring closure reaction, there is such a set of guidelines. In the mid 1970's, Dr. Jack Baldwin proposed what have become known as Baldwin's Rules For Ring Closure.<sup>1</sup> These rules will be addressed in further detail in this report. These rules are correct for a large number of systems, but are qualitative in nature and are generalized and cannot correctly predict every system. The goal of this research is to develop a quantitative model for two types of intramolecular ring-closure reactions. That is, a computer model is constructed employing all levels of computational methods. This model allows reactivity predictions that can be compared against

Baldwin's Rules. The reactions studied are the lactonization and the intramolecular Michael addition.

## II. Background: Computational Chemistry.

Computational methods can be used to predict the reactivity of certain chemical species. Utilization of computational methods reduces costly laboratory chemical experimentation and can save synthetic chemists time when preparing complex chemical compounds. Computational analysis has become a very prominent branch of chemistry during the past twenty years, and its applications extend to every other branch of chemistry. The validity of computational methods has been established by comparison to experimental results. A computational chemist who writes such programs as used here collects relevant experimental data and incorporates it into a model; this model is applied to specific chemical systems to obtain data consistent with other experimental results. The ultimate goal of this type of computational method is to be consistent to the point where it can be employed as a predictive tool. A computational model is considered useful when it can successfully predict chemical properties such as reactivity for several species, especially species that differ from those used to create the model.

In this research, a model for predicting the reactivity of ring closure reactions of the Baldwin Series type is developed. For a given chemical species, semi-empirical

methods are used to generate an optimized geometry. A geometrically optimized species is one in which no bond lengths or angles, or any other aspects of the species, could be changed to produce a configuration which is lower in total energy. It is important to note that the geometry of the species optimized at the semi-empirical level may not be the same geometry that an *ab initio* optimization would produce. It would be desirable to perform all optimizations at the highest level of *ab initio* theory possible; however, this is often not possible due to CPU time constraints and disk space requirements. A common practice is to perform geometry optimizations at the semi-empirical level or at a lower *ab initio* level. Then, an energy calculation is performed on this optimized species at a higher level of *ab initio* calculation. When energies for two species (such as a reactant and a reaction intermediate) have been obtained, it is the goal of this research to match this energy difference to that obtained from a molecular mechanics program. This involves developing parameters for chemically excited species. Parameterization has been done for several species in their ground states, but not for reaction intermediates, such as protonated species, or for transition states. It is important that parameters be developed for use in molecular mechanics programs for these types of species. Synthetic organic chemists do not normally have the resources or time to run semi-empirical or *ab initio* calculations when they want to

make reactivity predictions. It is common, however, for synthetic organic chemists to have access to molecular mechanics software. Molecular mechanics energy calculations are extremely fast compared to semi-empirical methods or *ab initio* calculations. Molecular mechanics software is also very user-friendly (menu-driven) and requires little experience in computational chemistry. The model developed here strives to make a quantitative molecular mechanics model for predicting reactivity of certain ring closure reactions.

Computational chemistry has become a prominent field of study in the past two decades. During this time, computational chemistry has evolved from an obscure sideline for physical chemists into a tool used by chemists in all fields of instruction and research by both academic and industrial laboratories. Some applications of computational chemistry include: energy determinations for simple molecules, modeling of transition-states and intermediates, tracking or determining reaction pathways, and identifying geometrical conformers of chemical structures. Proper implementation of computational chemistry in the laboratory can be an invaluable tool for synthetic organic chemists.

Computational methods may be divided into three specific categories: *ab initio*, semi-empirical, and molecular mechanics or force field methods. The most rigorous of these methods are of the *ab initio* type, which consider all electrons of the system. Semi-empirical techniques treat only valence

electrons, and are thus less mathematically complex than *ab initio* techniques. Molecular mechanics methods, on the other hand, do not consider electrons as such. These schemes treat molecules as ball-and-stick models governed by a force field based only on classical physics. The theory of molecular mechanics is much less abstract than the concepts employed in *ab initio* or semi-empirical techniques. These three methods will be addressed extensively to provide a sufficient background for the understanding of this research.

#### IIA. Computational Chemistry: Ab Initio Methods.

The highest levels of computational analyses are the *ab initio* quantum mechanical calculation methods. *Ab initio* means "from first principles" and thus implies that these methods are the most rigorous and most fundamental computational methods available. The principle concerned here is the three-dimensional distribution of electrons around the nuclei.<sup>2</sup> Most *ab initio* methods are based on molecular orbital theory, which derives from approximations to the solution of the Schrödinger equation of quantum mechanics. The Schrödinger equation is the fundamental equation of quantum mechanics. In simplest form, the Schrödinger equation is

$$H\psi = E\psi$$

where  $H$  is the Hamiltonian operator and represents the total

energy of the system,  $E$  is the numerical value of the energy of a particular state, and  $\Psi$  is the wavefunction describing the state of interest.<sup>3</sup> This equation can describe any many-electron system, atom, molecule, or ion; however, the Schrödinger equation can only be solved analytically (exactly) for a very simple system. Molecular orbital theory represents a solution to this many-electron problem in terms of single-electron functions which are called molecular orbitals. Molecular orbital programs, such as the common GAUSSIAN series developed during the early 1970's, construct these molecular orbitals as Linear Combinations of Atomic Orbitals (LCAOs).<sup>3</sup> These atomic orbitals,  $\phi_i$ , are centered on the individual atoms of the molecule:

$$\Psi_j = \sum C_{ij} \phi_i$$

where the summation is over all of the atomic orbitals on all atomic centers within the molecule.<sup>3</sup> These orbitals use Gaussian functions to approximate the individual atomic orbitals, which are then used to construct the LCAOs. The actual set of atomic orbital functions  $\phi_i$  used is called the basis set. When Gaussian functions are employed, the basis sets are therefore of the class called Gaussian Type Orbital (GTO). The mere use of these GTO's to describe molecular orbitals by means of LCAOs is an approximation. This approximation improves as the number of GTOs used per atomic

center increases. For a given basis set and selected geometry, molecular orbital programs then determine the values of the coefficients  $C_{ij}$  that produce the lowest electronic energy. The approach used to find these coefficient values is known as Hartree-Fock theory (HF). HF theory varies the coefficients in an iterative process until the electronic energy reaches a minimum and the orbitals' coefficients stop changing.<sup>3</sup> In the HF approach each electron in the system "sees" an average field produced by the other electrons in the system. In many molecular orbital methods, the molecular orbital is obtained iteratively by solution of the Schrödinger equation until a self-consistent (non-changing) field of electrons is obtained. Methods employing this feature are termed Self-Consistent Field (SCF) methods.

Although no parameterization is used to fit these *ab initio* methods to experimental data (as with semi-empirical or molecular mechanical methods), there are a variety of approximations which are commonly made in order to accommodate the practical requirements of computational facilities. The Hartree-Fock theory itself is an approximate solution to the Schrödinger equation within the Born-Oppenheimer approximation, which effectively freezes the position of the nuclei for each structure for which the molecular orbital is desired.<sup>2</sup> The LCAO approach is also an approximation.

The concept of the basis set is critical for understanding *ab initio* theory. By increasing the number of

basis functions (GTOs) the accuracy of the calculation is improved. The basis set selection significantly affects the molecular orbital calculation. For a given structure, the energy will always decrease with an increase in the number of basis functions employed.<sup>4</sup> However, there is a significant cost for this improvement. The time and disk space requirements of a computer's Central Processing Unit (CPU) increase roughly as  $N^4$  where  $N$  is the total number of basis functions used (Figure 1).<sup>4</sup>

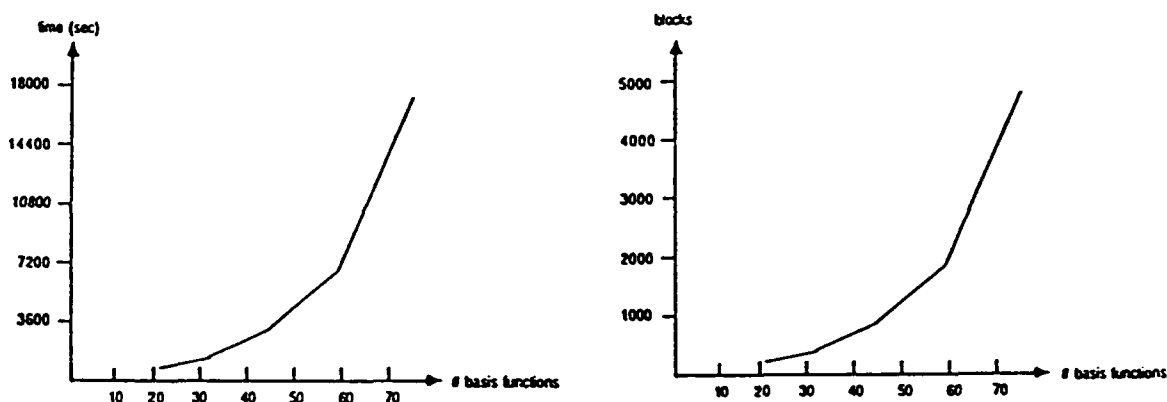


Figure 1.<sup>4</sup> CPU time (left) and disk space (right) required by GAUSSIAN versus the number of basis functions. Both CPU time and disk space required for the storage of 2-electron integrals increase roughly with the fourth power of the number of basis functions.

The simplest of the basis sets in GAUSSIAN is STO-KG (expansions of Slater-Type atomic orbitals in terms of K gaussian functions):

$$\phi_n(l,r) = \sum d_{n,l} g_l(\alpha_{n,l}, r)$$

where the subscripts  $n$  and  $l$  define the specific principal and angular quantum numbers,  $g_l$  are normalized gaussian functions, and  $d$  is the linear expansion coefficient.<sup>3</sup> The gaussians are of the form  $-ar^2$ ,  $\alpha$  being a constant determining the size of the function and  $r$  being the radial extent.<sup>3</sup> The most common of these "minimal basis sets" is the STO-3G calculation, which is used extensively for geometry optimizations on all sizes of molecular systems. These methods are referred to as "minimal basis sets" because they provide the minimum number of orbitals within a basis set necessary to accommodate all the electrons in the system and still maintain overall spherical symmetry.<sup>3</sup> Such basis sets are used to save disk space and CPU time when extreme accuracy is not required. The only notable disadvantage of these basis sets is their inability to adapt to different environments about an atom, such as solvation.<sup>3</sup>

The next level of basis sets used in *ab initio* calculations are the split-valence basis sets. Here, the atomic orbitals corresponding to the valence shell are split, such that there are two basis functions per valence shell orbital instead of one. Each of the basis function coefficients can then be optimized in the LCAO procedure.<sup>3</sup> Split-valence basis sets are designed to more accurately handle calculations for transition state metals through the

fourth row of the periodic table.<sup>3</sup> Such basis sets are typically written as  $n\text{-}21\text{G}$  or  $n\text{-}31\text{G}$  where  $n$  is the number of Gaussian functions used for the core orbitals (counted as a single function per core orbital) and the 21 and 31 describe how the valence shell orbitals are split ( $2$  Gaussians +  $1$  Gaussian or  $3 + 1$ ).<sup>4</sup> These are counted as 2 basis functions per valence shell orbital. Split-valence basis sets are used for determining the lowest energy conformation of a system when a higher level of accuracy is desired or when rough energies of the system are desired. Split-valence basis sets are more time consuming than the minimal basis sets and require increased disk space.

The highest level of basis sets for *ab initio* calculations include what are referred to as "polarization functions".<sup>4</sup> These are not normally involved directly in bonding, but rather allow the center of the  $p$ -orbitals to shift away from the atomic centers. The most common polarization function basis set used is the  $6\text{-}31\text{G}^*$  set, which uses 6 Gaussians for the core orbitals with a  $3/1$  split for the  $s$  and  $p$  valence shell orbitals. The asterisk (\*) indicates that a single set of  $d$ -orbitals is also included in the calculation.<sup>3</sup> The  $d$ -orbital considerations are important when determining the Hartree-Fock energy of a system and when analyzing electron correlation. Electron correlation attempts to define where electron density lies in relation to the atomic nuclei. Quantitative analysis of electron correlation

reveals important clues about the extent of bond formation for transition state structures. The polarization basis sets are employed when an accurate HF energy is required for an optimized geometry.

It is clear that a particular calculation of some specific property of a given molecular system can involve numerous variations of treatment. The final choice of which quantum mechanical model, basis set, and treatment of electron correlation should be used will ultimately depend not only on the established levels of performance, but also on practical considerations. The theoretician must compromise between quality of basis sets and time and computer resources available. Complete or partial optimization of geometrical variables need not always be carried out at the same level of theory required for the calculation of other properties.<sup>4</sup> Geometry optimization takes considerably more CPU time than single-point energy calculations. A common practice has been to obtain a partially- or fully-optimized structure at a relatively low level of theory (STO-3G or 3-21G), and then to use this geometry for a single calculation at a higher level, such as 6-31G<sup>3,5</sup>. While the performance of larger and more flexible atomic basis sets is desired, the most sophisticated methods cannot presently be applied to systems larger than approximately 10 atoms. Fortunately, even Hartree-Fock calculations with small basis sets [HF/STO-3G or 3-21G] often suffice in calculating certain properties. In these cases it

is not necessary to employ more sophisticated, higher level treatments.<sup>3</sup> Much time must be spent analyzing which method to employ based on cost effectiveness and level of theory desired, before running these calculations as they are costly and time consuming.

#### IIB. Computational Chemistry: Semi-Empirical Methods.

The next lower level of computational methods are the semi-empirical calculations. As opposed to *ab initio* calculations which treat all electrons in a system, semi-empirical calculations consider only valence-shell electrons. The nucleus and inner-shell (non-valence) electrons are effectively frozen and treated as a single unit. Further approximations are introduced in these programs by ignoring large numbers of integrals describing electron interactions or replacing them with empirical parameters.<sup>6</sup> Parameterization is carried out to fit experimental results derived from calculations of vibrational spectra, thermodynamic quantities, and kinetic effects.<sup>6</sup> Parameters thus cannot be better than the experimental data from which they are derived. They also tend to describe "average" behavior of specific model compounds. The result of the parameterization and "frozen core" assumptions is a less rigorous and less time consuming calculation. Figure 2 shows the CPU time required for a typical semi-empirical calculation versus the number of atoms in the molecule of interest.

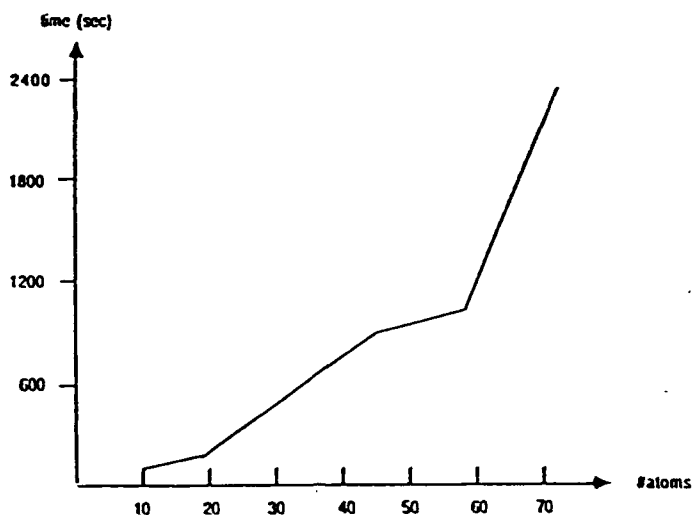


Figure 2.<sup>4</sup> CPU time required by MOPAC versus number of atoms. CPU time depends on the computer being used, but the relationship curve should remain the same.

The relationship is generally the same as that for *ab initio* methods, but less CPU time is required. The disk space required is also significantly less than that required for *ab initio* calculations.

The most widely used semi-empirical molecular orbital program is MOPAC, which is a general-purpose program that can be used to study chemical reactions involving molecules, ions, and linear polymers.<sup>6</sup> MOPAC is actually a collection of four semi-empirical methods, each distinguished by the Hamiltonian operator employed. The Hamiltonians currently available are MNDO, MNDO/3, AM1, and PM3; each of which was developed in order to overcome deficiencies of the previous method.<sup>6</sup> The four methods within MOPAC have many features in common. They are all self-consistent field (SCF) methods, they take into account electrostatic repulsion and exchange stabilization,

all calculated integrals are evaluated by approximate means (including parameterization), and they all use a restricted basis set of one  $s$  and three  $p$  orbitals ( $p_x$ ,  $p_y$ , and  $p_z$ ) per atom.<sup>6</sup>

A complete knowledge of these methods is not necessary to use MOPAC, but an understanding of how they differ from *ab initio* methods is important for the proper analysis and application of their results.

Semi-empirical calculations ignore integrals in the orbital overlap (secular) equations. Whereas rigorous quantum mechanical methods solve the equation

$$|\mathbf{H}-\mathbf{E}\mathbf{S}|=0,$$

semi-empirical methods solve for

$$|\mathbf{H}-\mathbf{E}|=0$$

where  $\mathbf{H}$  is the secular determinant,  $\mathbf{S}$  is the orbital overlap matrix, and  $\mathbf{E}$  is the set of eigenvalues.<sup>6</sup> Neglect of orbital overlap is the principal approximation in semi-empirical methods and considerably simplifies quantum mechanical calculations on the system of interest, thus allowing the study of larger systems. Therein lies the strength of semi-empirical methods: they are accurate enough to have useful predictive powers, yet fast enough to allow large systems to be studied.<sup>6</sup>

The principal use of semi-empirical calculations in this

research is to perform geometry optimizations and calculate heats of formation ( $\Delta H_f$ ) for molecular structures. MOPAC employs the BFGS (Broyden-Fletcher-Goldfarb-Shanno) method of geometry optimization.<sup>6</sup> This method calculates an initial energy for a given molecular structure. The geometry is then changed so as to lower the heat of formation by analyzing derivatives of the energy with respect to the internal coordinates of the molecule. When no further change can significantly lower the heat of formation, the geometry optimization is stopped.<sup>6</sup> This geometry corresponds to a stationary point on the potential energy surface containing differing molecular configurations of the molecule of interest. The optimized geometry is the one for which no distortion would lead to a decrease in the heat of formation. This configuration is assumed when any one of three criteria is met: 1) The predicted change in geometry is sufficiently small, 2) The predicted change in heat of formation is sufficiently small, or 3) The gradient norm is sufficiently small.<sup>6</sup> Any of these criteria can be changed, depending on the level of precision desired. Once again, the costs for higher precision are increased CPU time and a greater disk space requirement.

Semi-empirical methods are widely used due to their relative speed, compared with *ab initio* methods. Semi-empirical methods can sometimes even be used with more accuracy than *ab initio* methods. *Ab initio* methods must

predict accurately the energies and carry out quantum mechanical calculations from these fundamental, rigorous principles. The simplest levels of *ab initio* theory are sometimes inadequate due to their limited basis sets. The highest levels of *ab initio* could theoretically give the most reliable results, but it is not always practical to perform these calculations due to CPU time constraints and computer facility limitations. Semi-empirical methods may sometimes be more accurate than *ab initio* methods for systems similar to those for which they are parameterized, whereas *ab initio* methods are more likely to be accurate for other systems for which experimental evidence is currently lacking.<sup>6</sup>

### IIC. Computational Chemistry: Molecular Mechanics.

The third method of computational chemistry is referred to as molecular mechanics. Molecular mechanics is conceptually simpler and mathematically easier to employ than either *ab initio* or semi-empirical methods. Whereas *ab initio* and semi-empirical methods are specifically based on a system's electrons, molecular mechanics is relatively free of the extensive mathematical functions needed to describe these electrons. The greatest virtue of molecular mechanics is speed. If a scientist wants to study a certain molecule, he or she can do so by following one of two paths: experimental or theoretical. Experimentally, the scientist has to synthesize, separate, purify, and then (assuming it is in a

suitable form, i.e., solid for x-ray crystallography, gaseous for microwave or electron diffraction), analyze the molecule for the desired property. Theoretically, the scientist may perform quantum mechanical computations for the molecule. However, large amounts of time and extensive, complicated computer systems are needed for this type of study. Alternatively, a molecular mechanics calculation is orders of magnitude faster than a molecular orbital calculation. This factor alone makes molecular mechanics increasingly popular in industry (for study of large molecular systems such as drugs or polymers) and academia. Molecular mechanics is much easier to understand conceptually than quantum mechanics. The total energy is broken down into terms like compression and bending, which are more easily visualized than the mathematical concepts of quantum mechanics. Molecular mechanics is suitable for graduate and undergraduate curricula because it can quantitatively address questions such as steric hindrance, conformational analysis, and bond angle deformation. This method can quantitatively address many of the structural features traditionally shown by classroom models. More importantly, molecular mechanics has several research applications. The application being investigated here is to determine how results from high level, complex calculations can be integrated into a molecular mechanics package so it can be used as a predictive tool for ring closure facility. This model could save synthetic organic chemists a great deal of

time when planning syntheses and cut down on chemical waste when performing these syntheses.

Molecular mechanics is based on classical, simple harmonic motion. It considers a molecule as a collection of masses held together by springs, and, by applying Hooke's Law, it is possible to calculate how much energy is involved in stretching and bending bonds from their equilibrium values.<sup>2</sup> Hooke's law is simply:

$$E = \frac{1}{2}kx^2$$

where E is the total energy, k is an empirically determined proportionality constant, and x is the displacement variable for the type of motion being considered. The x term can be expanded into (x-x<sub>0</sub>) where x is the position of an atomic degree of freedom at a fixed moment in time compared to x<sub>0</sub>, the equilibrium position of that degree of freedom. The equilibrium position of a bond or angle is the average distance or angle as found in a large number of molecular systems. Molecular mechanics therefore depends on the values chosen for the constants k and the equilibrium values x<sub>0</sub>. These values are referred to as "parameters." Parameters are empirically determined so as to give reasonable energies that match experimental results. The parameters determined cannot produce energies with a great deal of accuracy for all species in a given class, but they can give reliable energies for most

species, thus making relative reactivity predictions within a class possible. The parameterization of a force field relies heavily on experimental data collected over the years. Therefore, judicious choice must be made between good and bad data because the reliability of the method can be no better than the data used for parameterization.<sup>2</sup>

The goal of molecular mechanics is to formulate as "reliable a recipe as possible for reproducing the potential energy surface for movement of atoms within a molecule."<sup>7</sup> All of the Hooke's Law equations describing the different types of distortions within a system are referred to as the "force field." The molecule is treated as a collection of atoms held together by elastic or harmonic forces. These forces can be described by potential energy functions. The potential energy functions determine the energy introduced into the system by distorting features such as bond lengths or internal angles from their idealized values. The combination of these potential energy equations comprise the force field. The energy,  $E$ , of the molecule in the force field can be approximated by a sum of energy contributions arising from the distortions:

$$E = E_s + E_b + E_a + \cdots,$$

where  $E_s$  is the energy introduced into the system by stretching a bond from its idealized value,  $E_b$  is the energy

caused by bending internal angles away from their idealized values, and  $E_t$  is the energy caused by distortion of internal torsion angles. All of these quantities will be discussed further. The total energy,  $E$ , is sometimes referred to as the "steric" energy. It is the difference in energy between the real molecule and a hypothetical molecule where all structural values like bond lengths, etc., are at their idealized values.

The basic philosophy of molecular mechanics rests on the fact that the force field is a computational model for describing the potential energy surface for all internal degrees of freedom in a molecule. There are no rules concerning how many or what type of potential functions should be used. Therefore, several force fields have been developed. Different force fields have been parameterized (fit) to give excellent molecular geometries, relative conformational energies, heats of formation, and crystal packing arrangements.<sup>2</sup> Although it is relatively easy to define parameters for a single molecule, the parameterization must be able to give satisfactory results for related systems containing the same functional groups. The underlying point to be kept in mind when constructing a force field is that it should be made transferrable from one molecule to another. Force field parameters are selected to reproduce experimental data from some test compounds, but the ultimate goal is to apply them to additional compounds whose detailed three

dimensional structures are not as well known. This research employs Tripos Associates' MAXMIN2 force field using SYBYL molecular modeling software.<sup>8</sup> All further equations and parameters will refer to the MAXMIN2 force field unless otherwise noted.

An important consideration when analyzing the results of molecular mechanics calculations is that the energy resulting from the force field is not related to any measurable quantity, such as a heat of formation. The strain energy is only a measure of intramolecular strain relative to a hypothetical situation in which all bonds and angles are in their idealized, "strain-free" positions; it is not an absolute value. The strain energy of two molecules may be approximately the same, whereas their heats of formation may vary by a considerable amount.

The component terms in the energy equation will change, depending on their functional form and the choice of parameters. These parameters are based on experimental evidence and are fitted so that molecular mechanics results are consistent with experimental data. Molecular mechanics is an extremely powerful tool which can be used to make qualitative and quantitative predictions for several physical properties such as rotational barriers and conformer populations.<sup>2\*</sup>

A better understanding of molecular mechanics and the force field concept is possible if a few of the simplest

component terms are analyzed. The MAXMIN2 energy expression (force field) is comprised of five standard energy contributions and seven optional energy terms:<sup>4</sup>

$$E = \sum E_{str} + \sum E_{bend} + \sum E_{oop} + \sum E_{tors} + \sum E_{vdw} + \left[ \sum E_{ele} + \sum E_{dist\_c} + \sum E_{ang\_c} + \sum E_{tor\_c} + \sum E_{range\_c} + \sum E_{multi} + \sum E_{fieldfit} \right]$$

where the sum extends over all bonds, bond angles, torsion angles, and non-bonded interactions between atoms. A brief definition of each of the energy terms is given:

$E_{str}$	is the energy of a bond stretched or compressed from its equilibrium bond length.
$E_{bend}$	is the energy of bending bond angles from their equilibrium values.
$E_{oop}$	is the energy of bending planar atoms out of the plane.
$E_{tors}$	is the torsional energy due to twisting about bonds.
$E_{vdw}$	is the energy due to van der Waals non bonded interactions.

#### Optional Energy Terms

$E_{ele}$	is the energy due to electrostatic interactions.
$E_{dist\_c}$	is the energy associated with distance constraints. {When minimizing a structure's energy, the user may hold certain bonded or non-bonded distances, angles, or torsional angles constant.}
$E_{ang\_c}$	is the energy associated with angle constraints.

$E_{\text{tor}_c}$	is the energy associated with torsion angle constraints.
$E_{\text{range}_c}$	is the energy associated with range constraints.
$E_{\text{mult}}$	is the energy associated with MULTIFIT, a program within SYBYL.
$E_{\text{field fit}}$	is the energy associated with FIELD-FIT, another program within SYBYL.

The first four terms (bond stretching, angle bending, out-of-plane, and torsional energy terms) are the significant terms in the expression, both conceptually and numerically, and merit further discussion.

The *bond stretching energy term* is defined as

$$E_{\text{str}} = \sum_{i=1}^{N_{\text{bonds}}} \frac{1}{2} k_i^d (d_i - d_i^0)^2$$

where  $d_i$  = length of the  $i^{\text{th}}$  bond in angstroms (Å)  
 $d_i^0$  = equilibrium length for the  $i^{\text{th}}$  bond (Å)  
 $k_i^d$  = bond stretching force constant (kcal/mol·Å<sup>2</sup>)

As can be seen by the bond stretching energy term, Hooke's Law ( $E = \frac{1}{2} kx^2$ ) is simply expanded to meet the character of the variable distance, angle, etc. being considered. The bond stretching force constant is one of the primary parameters in any force field. This parameter quantitatively describes how "strong" a bond is. The greater the stretching constant, the greater the bond strength and the more difficult it is to distort it from its equilibrium bond length,  $d_i^0$ . For example, MAXMIN2 parameters for single and double carbon-carbon bonds are 633.6 and 700 kcal/mol·Å<sup>2</sup>, respectively. The

equilibrium bond length is taken to be the average bond length for a number of molecules containing the particular bond of interest. While determination of these parameters is dependent on good experimental data, it is paramount to have a comprehensive knowledge of bonding theory and energy considerations. For example, if a bond is stretched 10% away from its idealized position, and an angle is skewed 10% from its idealized position, the energy introduced into the system by stretching the bond is approximately 10 times greater than the energy introduced by distorting the angle. Therefore, if a molecule is deformed it is expected that most of the distortion is in the bond angles rather than the bond lengths.

The angle bending energy term is defined as

$$E_{\text{bend}} = \sum_{i=1}^{N_{\text{angles}}} \frac{1}{2} k_i (\theta_i - \theta_i^0)^2$$

where  $\theta_i$  = angle between two adjacent bonds ( $^{\circ}$ )  
 $\theta_i^0$  = equilibrium value for the  $i^{\text{th}}$  angle ( $^{\circ}$ )  
 $k_i$  = angle bending force constant (kcal/mol $\cdot$ deg $^2$ )

Here, Hooke's Law is modified to fit angular displacement. The displacement variable  $x$  is now  $(\theta_i - \theta_i^0)$ , indicating that deviations from ideal bond angles increase the total energy of the system. This angle is defined by three atoms and is also referred to as a "valence" angle. An example is the common 109.5 $^{\circ}$  angle of a tetrahedron or the 120 $^{\circ}$  angle of a trigonal planar system. An example MAXMIN2 value is that for the tetrahedral angle formed by three sp $^3$ -hybridized carbon atoms,

0.024 kcal/mol·deg<sup>2</sup>

The *out-of-plane bending* energy term is defined as:

$$E_{oop} = \sum_{i=1}^{N_{oop}} \frac{1}{2} k_{oop,i} d_i^2$$

where  $d_i$  = distance between the center atom and the plane of its substituents (Å) {see Figure 3}  
 $k_{oop,i}$  = out-of-plane (oop) bending constant (kcal/mole·Å<sup>2</sup>)

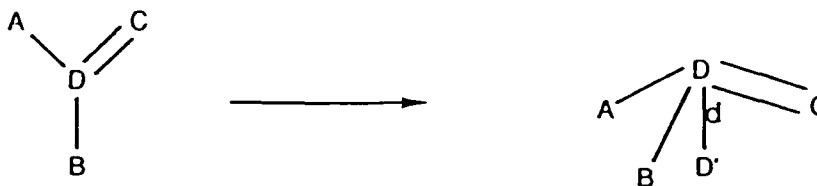


Figure 3. For out-of-plane (oop) bending at trigonal atoms (e.g.,  $sp^2$  and aromatic atoms),  $D'$  is a projection of the trigonal atom  $D$  on the plane formed by atoms  $A$ ,  $B$ , and  $C$  bonded to  $D$ .

For the out-of-plane bending case, the displacement variable  $d_i$  is a simple linear distance, which is the distance the atom of interest is removed from the plane. Out of plane bending force constants are significantly greater than those for the angle bending energy term, approaching the values for bond stretching parameters. This term is important for systems containing  $\pi$ -bonds because there is a large energy increase when these systems are distorted. Typical values in the MAXMIN2 force field are those for aromatic and  $sp^2$ -hybridized carbon atoms at 630 and 480 kcal/mol·Å<sup>2</sup>, respectively.

The torsional energy term also warrants analysis.

Torsion angles are concerned with internal rotation about a bond. Terms synonymous with torsion angles are "dihedral" or "twist" angles. Torsion angles are much easier to visualize than to describe. For molecule ABCD (Figure 4), the torsion angle is defined as the angle measured about the BC axis from the ABC plane to the BCD plane.<sup>2</sup>

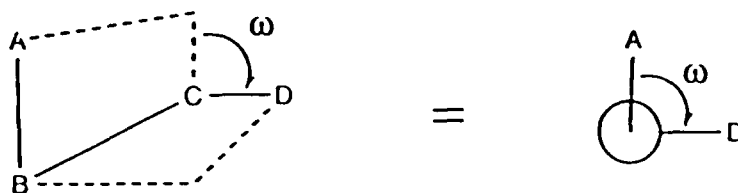


Figure 4. Torsion angle  $\omega$  for molecule ABCD is defined in the clockwise convention looking down the BC bond axis.

The torsional energy term is defined as:

$$E_{\text{tor}} = \sum_{i=1}^{N_{\text{tor}}} \frac{1}{2} V_i^{\omega} [1 + S_i \cos(|n_i| \cdot \omega_i)]$$

where  $V_i^{\omega}$  = torsional barrier (kcal/mol)  
 $S_i$  = +1 minimum energy when staggered  
           -1 minimum energy when eclipsed  
 $n_i$  = periodicity  
 $\omega_i$  = torsion angle ( $^{\circ}$ )

Simple inspection reveals that this energy term is much more complex than the previous expressions. This "barrier to rotation" energy term is described by the first two terms of a Fourier series.<sup>9</sup> The force constant  $V_i^{\omega}$  tells how difficult it is to distort this angular relationship from its equilibrium value. This term becomes extremely important when

modeling transition states to ensure that both electronic and geometric requirements are being met. These four primary energy terms (and other optional energy terms if included by the user) comprise the force field used to make energy determinations for molecular conformations.

#### IID. Energy Minimization and Conformational Analysis.

The force field is used to find molecular conformations which are lowest in energy. The energy is a function of the atomic coordinates and molecular mechanics programs attempt to generate the coordinates which correspond to a minimum of energy. This procedure is known as *minimization* or *optimization*. All minimization methods currently used for this purpose are called "descent series methods", which are iterative routines in which the atomic coordinates are modified from one iteration to the next in order to decrease the energy.<sup>10</sup>

Several optimization methods are available. One method is the "atom by atom" technique, where three cartesian coordinates of an atom are optimized simultaneously. Other methods optimize the orientation of groups of atoms as a whole, where the internal coordinates within a group are left unchanged. Some methods perform simultaneous optimizations on internal coordinates specified by the user, such as torsion angles.<sup>3</sup> The atom-by-atom method was employed in this research.

There are several mathematical methods for finding the minimum of a function. They can be classified as those using no derivatives, those using first derivatives only, and those using first and second derivatives. MAXMIN2 uses a combination of first- and non-derivative methods.<sup>3</sup> Non-derivative methods are often used on initial geometries where there may be severely distorted internal coordinates.

The Simplex method, a non-derivative procedure used to explore the potential energy surface, is used on an atom-by-atom basis until the maximum force on any atom is below some specified, user-defined value.<sup>11</sup> The potential energy surface and its derivative are often discontinuous when large, random "jumps" are made on the surface since internal coordinates can differ greatly in different areas of the surface. Whereas a derivative-based method would fail to complete optimizations for these structures, Simplex can handle such cases.<sup>10</sup>

After this initial minimization, MAXMIN2 uses a first derivative method. This is the primary optimization method for the MAXMIN2 force field. These first derivative optimizations employ procedures known as line searches. During a line search, a direction in n-dimensional geometric space in relation to the structure's current position is chosen. A sequence of steps in that direction is then taken until an energy minimum "bracket" along this direction is found. Then, a quadratic interpolation is performed until the energy minimum is isolated, meeting the user-defined accuracy

thresholds.<sup>10</sup>

Minimization procedures are very good at finding geometries with energy minima. However, an important concept to consider when performing minimizations is that of local versus global minima. The distinction between local and global minima can be readily understood by a quick analysis of three of the conformations of cyclohexane,  $C_6H_{12}$ .

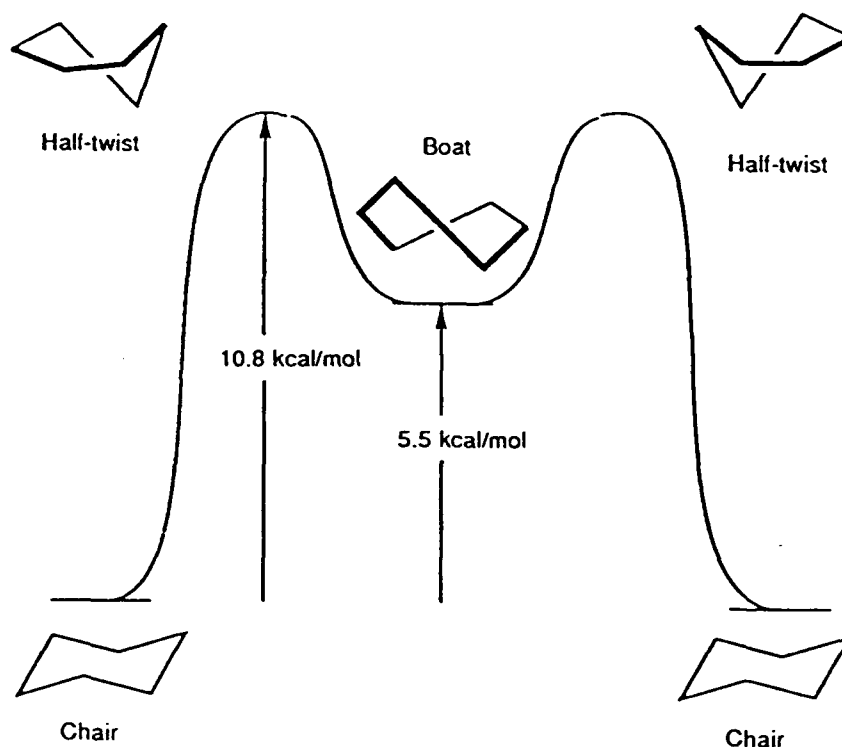


Figure 5. Energy diagram for most common conformations of cyclohexane.

The most stable conformation (geometrical configuration) of cyclohexane is the "chair" conformation. There are also other conformations of cyclohexane that are thermodynamically less

stable. These include the "boat" and "half-twist boat" conformations. The conformations and their relative energies are shown graphically in Figure 5.

The particular structure among the local minima that the minimization procedure will generate is totally dependent on the structure input by the user. If the starting geometry is near the lip of some potential energy well, the molecule will effectively "slide down" the potential energy surface during the minimization until it reaches the bottom. However, there may be a potential well on the surface which is even deeper. The deepest well represents the conformation with the lowest relative energy, or the global minimum. If the input starting geometry does not resemble the global minimum, the structure may minimize into one of the more shallow wells, or local minima. When comparing relative energy differences for a series of molecules, it is essential that the global minimum of each structure be used as a reference. Otherwise, reactivity and conformational population predictions may be worthless.

For small systems, most minimization procedures will find the global minimum. Geometries can be input manually using known experimental bond lengths and angles or results from *ab initio* or semi-empirical calculations. For larger systems, however, this becomes extremely difficult and time consuming. To determine the starting geometries for minimizations of large systems, conformational searches are performed.

Most approaches to conformational searching operate as follows:<sup>12</sup>

1. A crude starting geometry is produced and its structure is optimized by a molecular mechanics energy minimization.
2. This resulting minimum energy conformer is compared with previously found conformers. If it is unique, it is added to a list of conformers; if not, it is discarded.
3. The cycle is repeated by obtaining a new crude geometry, followed by a molecular mechanics energy minimization, etc.
4. When all starting geometries have been used, or new minima cease to be found, the search is terminated.

The molecular mechanics energy minimization part of the process simply refines the starting geometries to the nearby local minima. Therefore, it is the algorithm that generates the starting geometry which "most directly controls the overall effectiveness of the search in reaching convergence."<sup>12</sup>

Two prevalent categories of methods are used to generate starting geometries for conformational searches: deterministic (systematic) searches and stochastic (random) searches. The systematic search covers all of conformational space. The systematic search is a "grid search" conducted by systematically altering internal coordinates. All combinations of selected values for some or all rotatable torsion angles are generated to produce starting geometries distributed throughout conformational space.<sup>12</sup> The set of

rotatable bonds and the size of the "grid" are determined by the user. The principal advantage of a systematic search is that it provides guaranteed coverage of all regions of space. If the calculation is allowed to run long enough, the global energy minimum will eventually be found. However, this procedure is extremely time-consuming because of the number of structures it generates. Also, if the number of values allowed for each torsion is small, then "the resolution with which space is covered may be inadequate to provide a starting geometry in the vicinity of each minimum."<sup>12</sup> This may result in the global minimum being missed.

The random search (also known as stochastic or Monte Carlo search) generates starting geometries using random variations of molecular geometry. Contrary to the name, this method does not search conformational space in a completely random manner. Random searches start with stable conformers and limit their conformational space explorations to variations in selected internal coordinates or to small (<3.5 Å) cartesian displacements of atoms from the previous conformation found in the search.<sup>12</sup> Random searches provide significant advantages. Most important to the user is the decreased time requirement compared to systematic searches. Even though random searches do not go about their exploration of conformational space "systematically", they are by nature a more comprehensive method and can be used to search conformational space as extensively as necessary to reach (in

principle) any desired degree of convergence.<sup>12</sup> Although faster than systematic searches, random searches still take considerable amounts of CPU time. A molecule containing 10 to 15 atoms could take 2 to 24 hours, depending on the degree of convergence desired and the structure involved. Measures can be taken to limit the scope of the search and thus reduce the required CPU time. Known torsional angles, bond lengths, conjugated arrangements, and other stereoelectronic requirements can be held constant throughout the search, significantly decreasing the degrees of freedom within the molecule.

### III. Transition State Theory and Activation Energy.

Before discussing the exact systems of interest in this research, two fundamental concepts must be understood: transition states and activation energy.

During a chemical reaction, a reactant species goes through a chemical transformation either intermolecularly (with another species) or intramolecularly (within the species itself). In the course of the reaction, two things can happen: a reaction intermediate is formed or a transition state is reached. Whereas a reaction intermediate can be observed and studied, a transition state is short-lived (on the order of  $10^{-12}$  sec) and cannot be directly observed or studied. Since this species has such a short lifetime, it cannot be studied using analytical techniques. Consequently,

all information about transition states is indirect or obtained by theory. The free energy required for attainment of the transition state is known as the *free energy of activation*, or *activation energy*. The rate at which a reaction occurs is related to the height of this activation energy hill. A high energy barrier represents a slow reaction rate, whereas a lower energy barrier represents a faster reaction rate.

Transition states and reaction intermediates can be understood qualitatively by illustration with potential energy diagrams. Shown in Figure 6 are diagrams for a hypothetical one-step bimolecular reaction and a two-step reaction. Such diagrams make clear the difference between a transition state and a reaction intermediate. The line in each diagram traces the free energy of the reaction complex as it progresses along the reaction coordinate from reactants to products. The lower diagram depicts a two-step reaction. Point C is a reaction intermediate and has a finite lifetime. Intermediates lie in a depression on the potential energy curve. The actual lifetime of the intermediate depends on the depth of the depression. A shallow depression implies low activation energy for the subsequent step and therefore a short lifetime. The deeper the depression, the longer will be the lifetime of the intermediate.<sup>13</sup> A transition state has an extremely short lifetime and is represented by a maximum on the reaction path. In the bottom figure, there are two transition states. The

first transition state has a higher activation energy than the second, implying that it is the slower (i.e., rate determining) step of this particular reaction mechanism.<sup>13</sup>

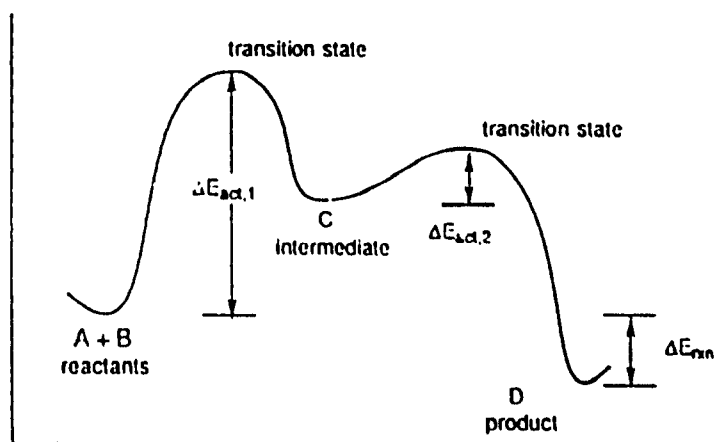
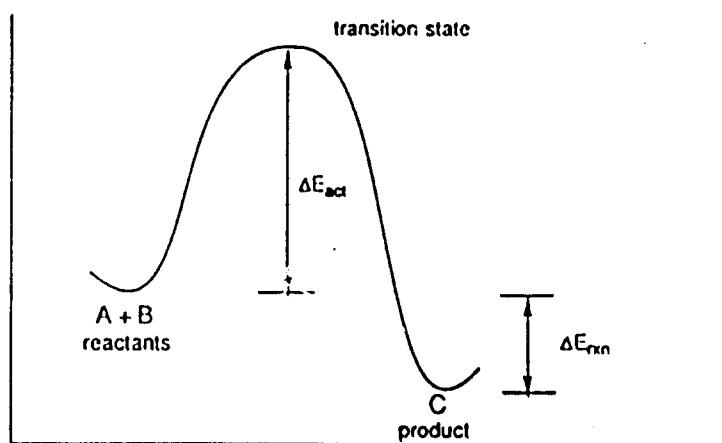


Figure 6.<sup>13</sup> Potential energy diagrams for single-step and two-step reactions. These diagrams show the difference between reaction intermediates and transition states.

The energy plots in Figure 6 are actually two-dimensional "slices" of a three-dimensional potential energy surface. In any chemical reaction, there is one path between reactants and products on this three dimensional surface that has a lower energy maximum than any other. This is the pathway the reaction will follow and the line in a two-dimensional energy plot represents this lowest-energy pathway.<sup>13</sup> Thus, a transition state can be viewed as a saddle-point on a potential energy surface. It is important to note that the same pathway that is traveled in the forward direction of a reaction will likewise be traveled in the reverse direction, traversing the same transition state. This is known as the *principle of microscopic reversibility* and implies that for a reversible reaction, the transition state of the forward process is identical to the transition state of the reverse process.<sup>13</sup> The transition state and activation energy concepts, along with the principle of microscopic reversibility are fundamental to this research. The model developed predicts reactivity for a certain class of reactions; the difference in energy between a reactant and the transition state (the activation energy) is directly related to this reactivity.

#### IV. Approach.

Methods of computational chemistry are being employed to model transition state structures for certain classes of chemical reactions. For a given intramolecular reaction, *ab initio* or semi-empirical calculations are performed on a similar intermolecular reaction (containing reacting centers similar to the intramolecular reaction) in order to determine the transition state structure's geometry. These geometrical values for transition state bond distance and bond angles are then used to define molecular mechanics atom types for transition states for that class of reaction. The force constants needed to define the bond and angle strengths are not directly available from the semi-empirical or *ab initio* calculations and must be determined analytically. Known transition state structures are then built, implementing these parameters. These structures are then minimized, and reactivity predictions can be made by comparing the energy difference between reactants and transition states for a series of similar reactions. Comparison and fitting of these reactivity trends to the known trends by adjusting the parameters fine tunes the model. Further validation of the parameters is accomplished by comparison to several systems which contain similar reaction centers and have available kinetics data for comparison. When it is determined that the parameters are general enough to predict reactivity trends for several similar systems, the model can be used as a viable

prediction tool for reactions for which no rate data is available.

## V. Experimental.

Specific reactions of interest are intramolecular ring closure reactions of the type addressed by Baldwin's Rules for Ring Closure.<sup>1</sup> Baldwin's Rules for Ring Closure are a set of rules which predict the relative facility of different ring closure reactions. Baldwin formulated these rules by conducting extensive searches in the chemical literature, investigating the effects of ring size, stereochemistry, and functional groups on the ability of a molecule to intramolecularly form a ring. The rules he determined are as follows:<sup>1</sup>

### Rule 1: *Tetrahedral Systems.*

- (a) 3- to 7-*Exo-Tet* are all favored processes.
- (b) 5- to 6-*Endo-Tet* are disfavored.

### Rule 2: *Trigonal Systems.*

- (a) 3- to 7-*Exo-Trig* are all favored processes.
- (b) 3- to 5-*Endo-Trig* are disfavored.
- (c) 6- to 7-*Endo-Trig* are favored.

### Rule 3: *Digonal Systems.*

- (a) 3- to 4-*Exo-Dig* processes are disfavored processes.
- (b) 5- to 7-*Exo-Dig* are favored.
- (c) 3- to 7-*Endo-Dig* are favored.

Baldwin's nomenclature is defined as follows:

numerical prefix- describes the size of the ring being formed.

Exo- when the breaking bond in the ring forming process is exocyclic to the smallest ring formed.

**Endo-** when the breaking bond in the ring forming process is endocyclic to the smallest ring formed.

**Tet, Trig, and Dig-** indicates the geometry of the carbon atom undergoing the ring closure reaction.

A few generic examples of Baldwin type ring closures with terms are given in Figure 7.

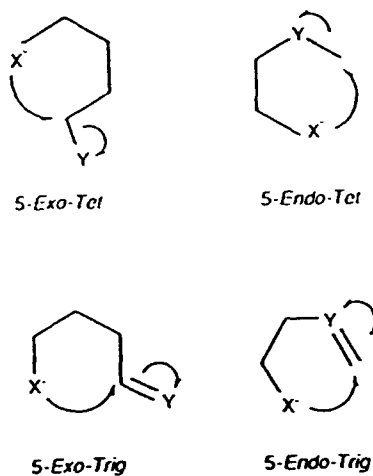
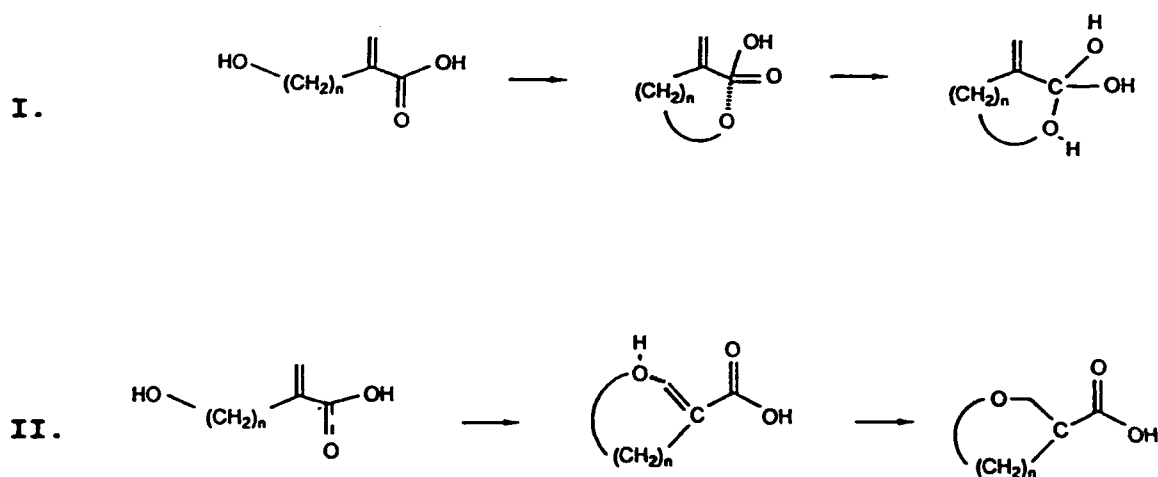


Figure 7. Generic ring closure reactions labelled with Baldwin nomenclature.

The overall goal of this research is to formulate a molecular mechanics model which will give the same relative reactivity predictions as Baldwin's empirically determined rules. This is accomplished by formulating force field parameters for reacting centers in the transition states of certain ring closures. A UNIX-based Silicon Graphics Iris-4D workstation employing Tripos Associates' SYBYL Molecular Modeling Software and the MAXMIN2 force field is used in this research. Using parameters developed for these transition states, reactivity predictions can be made for series of

reactions already addressed by Baldwin's Rules or already determined experimentally. Successful correlation with these rules will allow qualitative reactivity predictions for intramolecular reactions for which no experimental work has been reported.

Two classes of reactions are investigated in this research: lactonizations and Michael additions. Lactonizations involve nucleophilic attack at a carbonyl carbon center. Michael additions involve nucleophilic attack at the  $\beta$ -carbon of an  $\alpha,\beta$ -unsaturated system. The system of interest in this study could theoretically undergo either reaction because it has competitive reaction centers. Species for which the size of the ring being formed was 4- to 10-membered were studied (Scheme 2).



Scheme 2. Lactonization (I) and Michael addition (II) investigated in this study, where  $n$  ranges from 1 to 7.

An important consideration must be addressed: Can

transition state theory be used to explain this reactivity trend? The reaction path taken (lactonization or Michael addition) can depend on either of two factors: kinetics or thermodynamics. When a species is thermodynamically favored, it is simply lower in overall energy. Kinetics has to do with the "rate" at which a reaction will occur and is directly related to the activation energy of the reaction. In order to determine which factor controls this system, the kinetics and thermodynamics of the competing reaction pathways had to be investigated.

The thermodynamics were investigated first. The bifunctional reactant and the lactone and cyclic ether products in Figure 8 were constructed and energy determinations were made at the AM1 level for each species. First, each species was fully geometry optimized at the AM1 level to ensure that the lowest energy conformations were being compared. Then, AM1 heats of formation were obtained. The results show that the cyclic ether formed through the intramolecular Michael addition is lower in energy than the lactone formed through lactonization. This implies that if thermodynamics controlled product formation for this competitive reaction, the cyclic ether would be the only product formed. However, it has been shown experimentally (and Baldwin's rules predict) that the lactonization is the reaction which occurs for rings smaller than 6-membered. This suggests that the kinetics of this competitive reaction

controls product formation and transition state theory can therefore be used to determine reactivity.

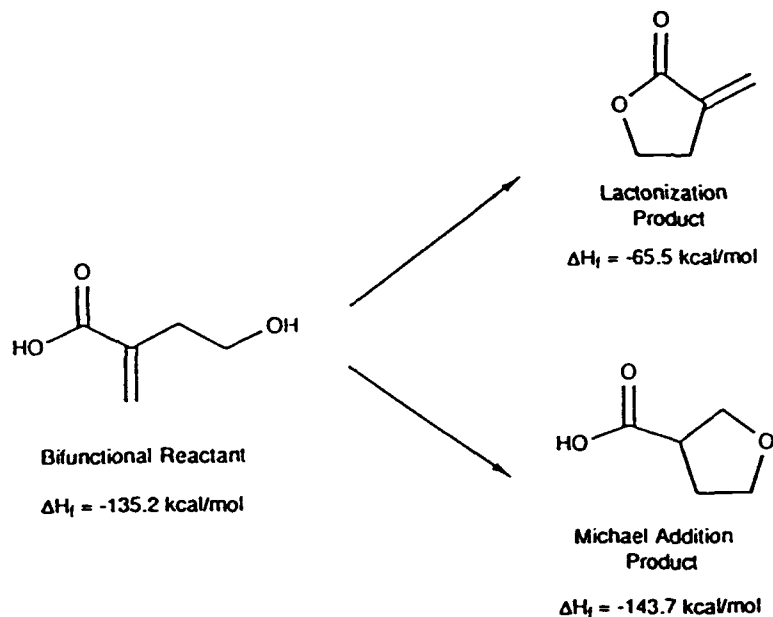


Figure 8. The Michael addition product is shown to be thermodynamically preferred over the lactonization product. Calculations were performed at the AM1 level.

Investigation of the kinetics of these competitive reactions requires a knowledge of their reaction mechanisms. Mechanisms for the systems being studied in this research are generally accepted as shown in Figures 9 and 10.

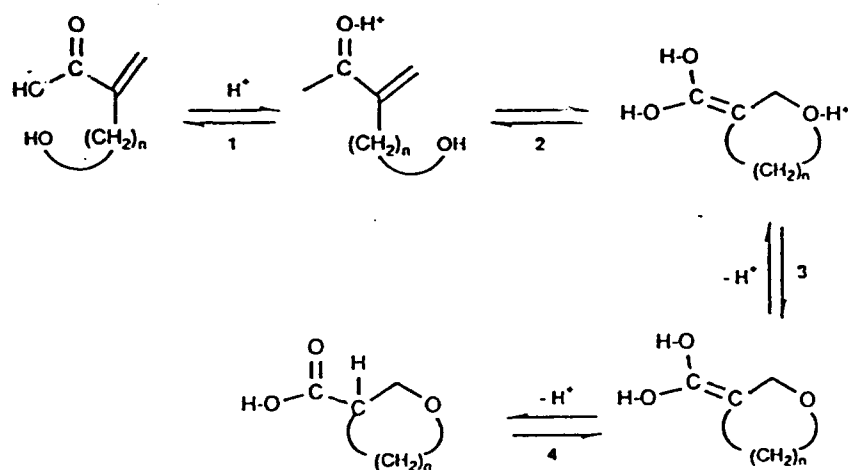


Figure 9. Accepted reaction mechanisms for the Michael addition investigated in this study.

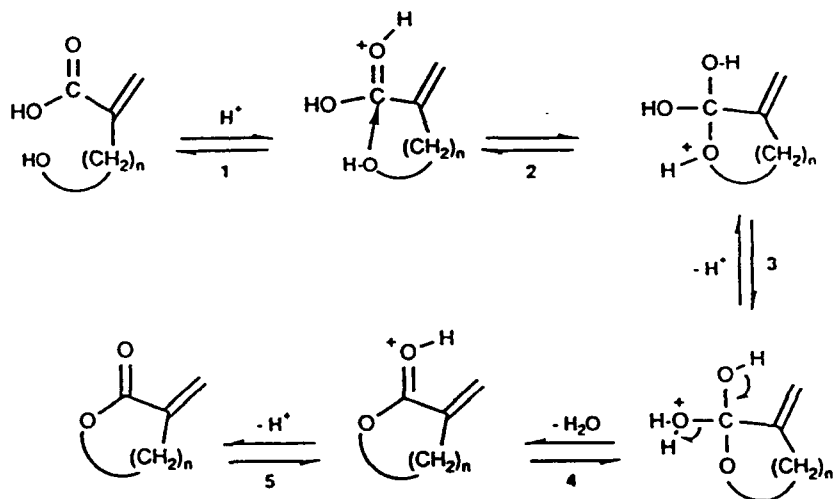


Figure 10. Accepted reaction mechanism for the lactonization investigated in this study.

In any reaction mechanism, there is one step that is more difficult to achieve than any other since the activation energy of that step is the greatest. This step is known as the rate determining step and determines the overall kinetics for the reaction. The rate determining step for Michael addition is step 2, the nucleophilic attack by oxygen on the  $\beta$ -carbon. The rate determining step for the lactonization is step 4, the loss of water from the cyclic ether. Since the energy difference between the reactant and the transition state determines if a reaction proceeds, both the reactant and the transition state structures are needed so that energy determinations may be made for these structures.

Since these systems are relatively large, it is unfeasible to determine the transition state geometries by *ab initio* or semi-empirical methods. A common practice is to use simpler intermolecular systems containing similar reaction centers as the larger intramolecular system.<sup>5,14</sup> The major advantage to employing these smaller systems is that they require much less CPU time. Also, the results obtained are more general. That is, they are not specific to the lactonization or intramolecular Michael addition being modeled; the results can be applied to other reactions with similar reacting centers. A third advantage is that conformational effects due to the connecting chain are avoided; the calculations are focused on the transition state of the reaction centers. This again aids in making the

results applicable to similar reactions.

The lactonization rate determining step was shown to be the loss of water from the tetrahedral intermediate (Figure 10, step 4). Based on the principle of microscopic reversibility, the transition state for this step can also be simulated by the addition of water to the carbonyl carbon of protonated formic acid.<sup>5</sup> The rate determining step for the intramolecular Michael addition was shown to be the nucleophilic attack by oxygen on the  $\beta$ -carbon (Figure 9, step 2). A simulated transition state for this step is modeled by nucleophilic attack of a water molecule on protonated acrylic acid at the  $\beta$ -carbon.

Structures of interest for both reaction mechanisms were optimized at AM1 level and subsequent energy determinations were performed at the AM1 level. From these calculations it is evident that the transition state for the simulated lactonization is lower in energy than the transition state for the simulated Michael addition. These results indicate that although the Michael addition is thermodynamically preferred, the lactonization is kinetically preferred (Figure 11).

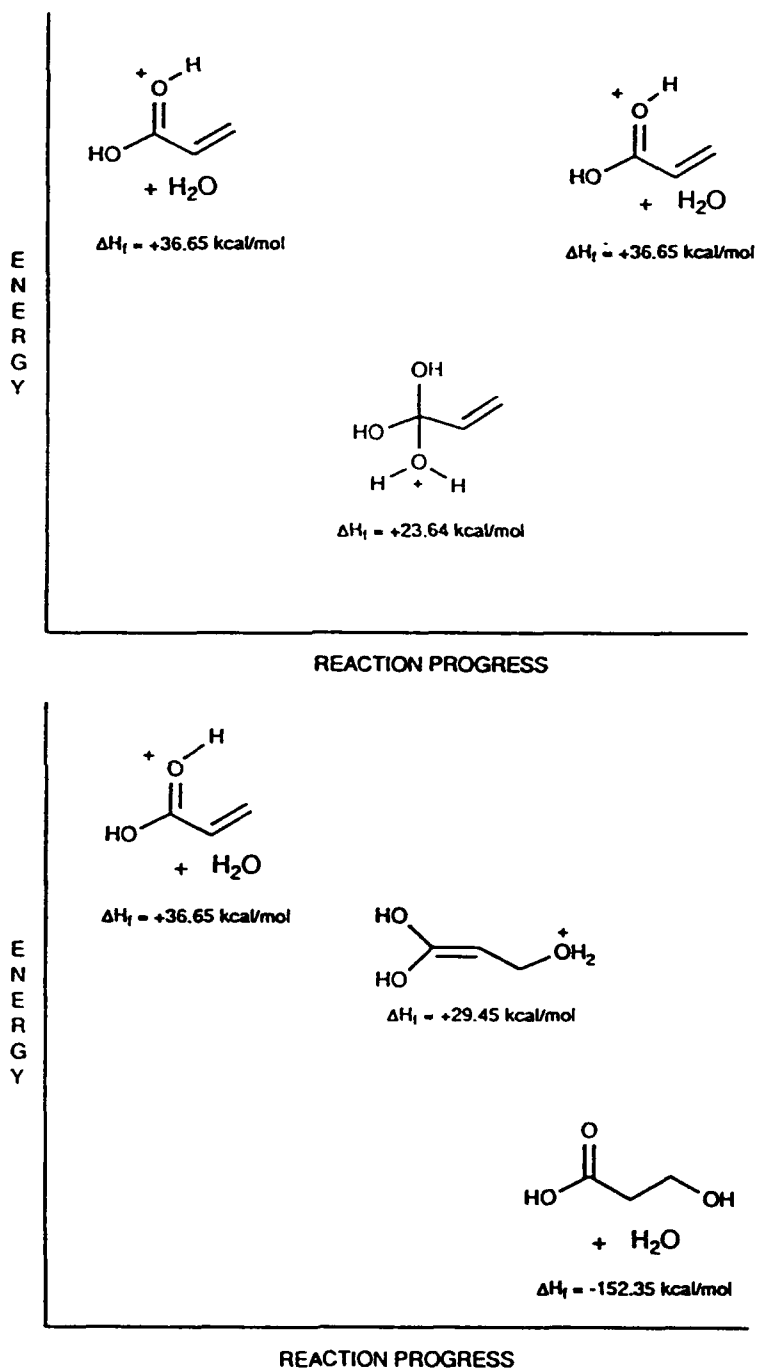


Figure 11. Relative Energies for Reaction Intermediates

Determination of the transition state geometry was performed as follows. The distance and angle between the reacting centers are systematically varied and an energy determination is made for each of these geometries. For a set distance, the energy should vary as the angle is changed. This energy reaches a minimum when the angle is in its preferred position. At that angle, the distance is also varied. As the distance is varied, the energy correspondingly changes, allowing the determination of the distance at which interaction and bond formation begins. The transition state can therefore be visualized as a "saddle point" on a three-dimensional grid of a potential energy surface.

A transition state for the nucleophilic attack by water on the carbonyl carbon of formic acid has been proposed by K.N. Houk (Figure 12).<sup>5</sup> Houk performed RHF/3-21G geometry optimizations followed by 6-31G single point energy determinations on structures in which the C--O distance (distance between the carbonyl carbon and the attacking oxygen) was constrained at different values while the rest of the molecule was allowed to optimize.<sup>5</sup> Houk found that there is a consistent, preferred geometry for this transition state. The C--O bond length was found to be approximately 2.05 Å and the O--C-O bond angle (angle formed by the carbonyl group and the nucleophilic oxygen) was found to be 97.4°.<sup>5</sup> These values imply that this is an "early" transition state. The average C-O bond length is approximately 1.43 Å, whereas the

transition state bond length was determined to be 2.05 Å. Also, the normal angle value at an  $sp^3$ -hybridized carbon center is  $109.5^\circ$ . The value in the transition state is  $97.4^\circ$ , indicating that the angle must change significantly before product formation.

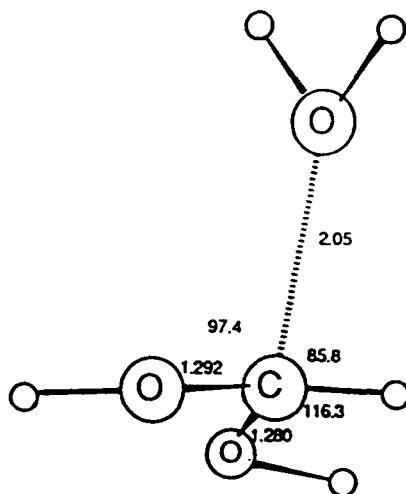


Figure 12. Simulation of lactonization transition state is shown by the nucleophilic attack of water on protonated formic acid as proposed by K.N. Houk.<sup>5</sup> Transition state bond lengths and angles are depicted.

Determination of the transition state geometry for the nucleophilic attack of water on the  $\beta$ -carbon of acrylic acid (Michael addition) was achieved using an approach similar to Houk's.<sup>5</sup> Geometry optimizations and energy determinations were done at the AM1 level. Although *ab initio* calculations give more accurate energies in some cases, they are extremely time consuming for the size of system investigated in this research. Semi-empirical calculations give reliable results

that can be used for determination of transition state geometries. The accuracy gained by employing *ab initio* methods is somewhat lost in the transition to the molecular mechanics model due to approximations that have to initially be made when determining force constants for the transition state geometrical parameters. Therefore, it was determined that AM1 calculations would give transition state geometries sufficient for the construction of this molecular mechanics model.

The forming bond distance and the angle of attack between the nucleophile and the  $\alpha,\beta$ -unsaturated system were systematically varied. All other bond lengths, valence angles, and dihedral angles were allowed to optimize for every combination of transition state bond distance and angle tested. Initial calculations were performed at the AM1 level by varying the angle of attack from  $90^\circ$  to  $120^\circ$  at increments of  $5^\circ$  while systematically varying the bond distance from 1.5 to 2.7 Å. The grid was subsequently narrowed down and energy determinations were made by varying the attack angle from  $105^\circ$  to  $110^\circ$  at increments of  $0.5^\circ$  while systematically varying the distance from 1.5 to 2.2 Å. Analysis of the resulting grid shows that there is an energy well in the  $106^\circ$  to  $108^\circ$  region, indicating the preferred angle of attack (Table 1).

DIST \ ANG	102	103	104	105	106	107	108	109	110
1.5	39.75	39.24	39.40	38.54	38.23	38.04	37.89	37.84	37.79
1.6	37.82	37.47	37.20	37.00	36.85	36.82	36.73	36.77	36.80
1.7	37.57	37.35	37.16	37.07	36.98	36.95	36.98	37.07	37.15
1.8	37.33	37.17	37.05	37.00	36.94	36.95	36.99	37.05	37.16
1.9	36.59	36.46	36.36	36.31	36.29	36.28	36.30	36.35	36.45
2.0	35.32	35.23	35.11	35.06	35.07	35.00	34.99	35.01	35.05
2.1	32.07	32.07	32.12	33.36	32.27	33.20	32.38	33.20	33.21
2.2	30.65	30.59	30.62	30.68	30.69	30.81	30.74	30.88	30.94

\* Energies are in kcal/mol

Table 1. Values are heats of formation given in kcal/mol. A saddle point is shown to exist between 106 and 108 degrees and between 1.6 and 1.9 Å.

As the distance is varied from 1.5 to 2.2 Å in the 106° to 108° region, there is a definite energy hill between 1.7 and 1.8 Å, indicating the transition state bond length. At distances greater than 1.8 Å, the energy decreases because there are less repulsive forces between the water molecule and the protonated acrylic acid; at distances closer than 1.7 Å, the energy decreases until the atoms are brought inside their equilibrium bond lengths. When the atoms involved in the forming bond are brought inside their equilibrium bond lengths, significant nuclear-nuclear repulsion effects rapidly elevate the energy of the system. Thus, the transition state

was determined to occur at 1.75 Å and 107°. Holding the transition state bond length at 1.75 Å and the angle of attack at 107°, the structure was geometry optimized at the AM1 level (Figure 13):

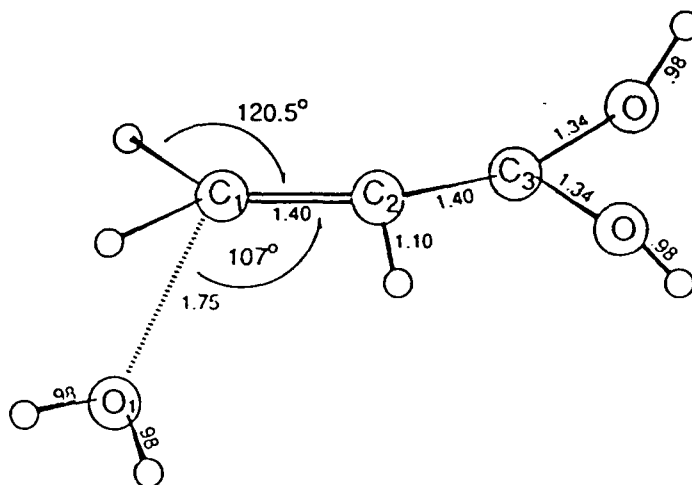


Figure 13. Simulation of Michael addition transition state structure is shown by the nucleophilic attack by water on the  $\beta$ -carbon of protonated acrylic acid. The transition state bond lengths and angles are depicted.

This transition state geometry provides some interesting results. The  $C_1$ - $C_2$  double bond in the protonated acrylic acid (prior to attack by water) is 1.35 Å. The  $C_2$ - $C_3$  single bond in the protonated acrylic acid is 1.48 Å. The transition state bond length for both bonds is 1.40 Å. The final product bond lengths for the  $C_1$ - $C_2$  and  $C_2$ - $C_3$  bonds are 1.51 Å and 1.34 Å, respectively. The equal transition state bond lengths for the  $C_1$ - $C_2$  and  $C_2$ - $C_3$  bonds are in between the values for single and double carbon-carbon bonds. These results imply that significant bonding rearrangement has taken place and that the

geometry is beginning to resemble the product geometry. This implies a "late" transition state. In this late transition state the C<sub>1</sub>-O<sub>1</sub> bond length is expected to be shorter (1.75 Å) than in an early transition state since extensive bond formation is occurring.

The high level calculation phase of the research provided transition state structures for simulated lactonization and intramolecular Michael additions. These geometrical values are now incorporated into a molecular mechanics force field and models for both transition states are constructed.

#### VI. Integration of Parameters Into Force Field.

The results of the *ab initio* and semi-empirical calculations are used to construct molecular mechanics models for these transition states. The procedure followed is similar to the one employed by Houk.<sup>5</sup> Important bond distances, valence angles, and torsional angles are extracted from the transition state geometries found in the *ab initio* and semi-empirical calculations. In these models, all bond lengths and angles involving the breaking or forming bonds are set equal to the corresponding values calculated in the *ab initio* or semi-empirical studies.<sup>5</sup> For example, two new atom types were defined for the MAXMIN2 force field. These two new atoms represent the oxygen and the carbon of the reacting center. The bond distance of 1.75 Å is set as the equilibrium bond distance in order to replicate the bond between the

reacting centers in the transition state of the Michael addition. All other geometrical parameters in the system are standard MAXMIN2 values. This procedure defines the geometry of the transition state, but does not determine the force constants for the bonds and angles which significantly change during the transition state.<sup>5</sup> Standard MAXMIN2 force constant values cannot be used to define the strength of these parameters, for they refer to equilibrium, non-transition state bonds. Therefore, new bending, stretching, and torsion constants which involve the breaking and forming bonds in the transition state were developed.

The force constants define the ease or difficulty with which a structure is distorted from its idealized geometry. When the geometry is distorted in the minimization procedure, these force constants determine the magnitude of the strain energy. Larger force constants indicate stronger bonds, or angular relationships which should be difficult to distort. When bonds or angles involving these parameters are distorted in the minimization procedure they lead to a large energy increase, indicating that their distortion is highly unfavored. Smaller force constants refer to weaker, partially formed bonds or "loose" angular relationships. When bonds or angles defined by parameters with small force constants are distorted in the minimization procedure they lead to a lesser energy increase, indicating that there is more flexibility in the system.

Determination of the optimum numerical values for the force constants is a difficult task, requiring in-depth analysis of structures minimized using the new parameters. Force constants already defined for ground state bonds and angles provide guidelines for the magnitude of the transition state force constants. In a transition state, nearly all bond lengths and angles change to some extent, even those not directly involved in the bonding centers. However, determination of force constants for every geometrical value that changes in a transition state would be unrealistic, at best. Therefore, only parameters for the bond lengths and angles directly involved in the forming or breaking bonds are developed.

Integration of Houk's transition state for the lactonization simulation was attempted first because his parameters have been validated for a different molecular mechanics package.<sup>5</sup> The lactonization parameters integrated into the MAXMIN2 force field are listed in Appendix A, table 1. A force constant of 309.5 kcal/mol·Å<sup>2</sup> was chosen for the transition state bond of 2.05 Å (C<sub>3</sub>-O, in figure 14). This force constant is one-half the value of a C(sp<sup>3</sup>)-O(sp<sup>3</sup>) force constant in the MAXMIN2 force field. This value was chosen since the rather long transition state bond length (2.05 Å) is a partially formed bond and is not expected to be as strong as a fully formed single bond. The MAXMIN2 default force constant values are used for all other bonds in the transition

state structure. The  $97.4^\circ$  angle of attack (angle  $O_8-C_3-O_9$ , in figure 14) was assigned a force constant of  $0.010 \text{ kcal/mol}\cdot\text{deg}^2$ , which is one-half the value of an  $O(\text{sp}^3)-C(\text{sp}^3)-O(\text{sp}^3)$  force constant. Again, this value was chosen since the angle will have a degree of flexibility due to the partially formed bond involved in defining the angle. The MAXMIN2 default force constants were used to describe all other angles in the transition state structure.

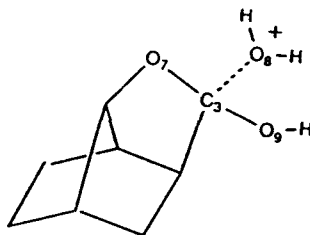


Figure 14. Atom types defined for lactonization transition state for the MAXMIN2 force field. Parameters are listed in Appendix A, Table 1.

Testing of these parameters determined for the MAXMIN2 force field was performed on a series of four molecules for which lactonization rate data was available (Figure 15). The reactant and proposed transition state for each reaction in the series was constructed using SYBYL molecular modeling software. The global minimum energy conformation was found for each structure utilizing a random conformational search, followed by minimization with the MAXMIN2 force field

employing the new parameters. The conformational search was utilized to ensure that the global minimum of each reactant was being used for comparison to the transition state rate data. If the energies used for one reactant were obtained from its global minimum geometrical conformation, but the energies obtained for other reactants were not global minima, the trends predicted by the energy differences may not match those determined experimentally. This could erroneously lead to the assumption that the parameterization is incorrect.

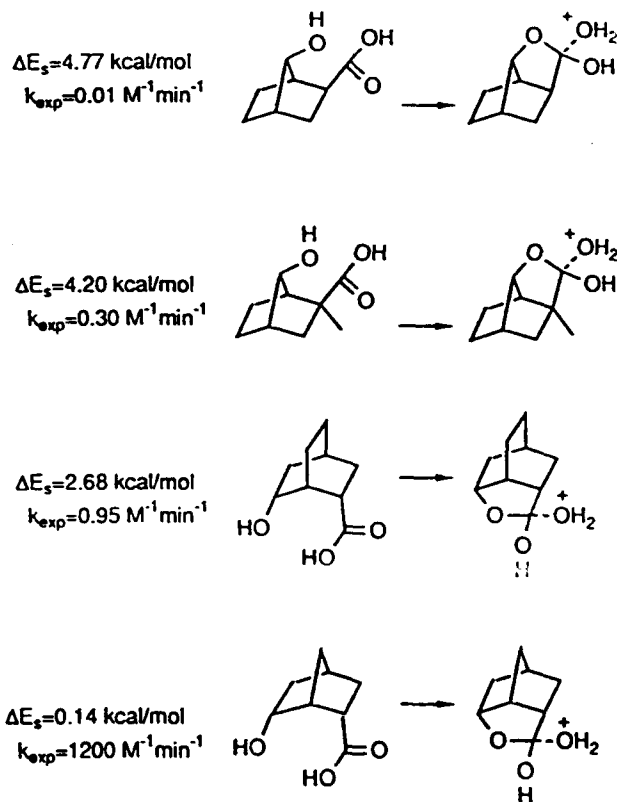


Figure 15. This series of molecules was modeled using parameters derived from Houk's transition state. The minimized energy differences between reactant and proposed transition state predict a similar trend to the experimentally determined rate data.

As the energy difference between the reactant and the transition state increases, the rate at which the reaction proceeds correspondingly decreases. The energy differences determined using these parameters correctly predicts the experimental reactivity trend. Further validation of these parameters will be accomplished by comparison to rate data for similar systems for which experimental rate data is available. It is important to note that the energy differences determined by molecular mechanics are strain energies (measuring the extent of deformation compared to hypothetical unstrained structures), not activation energies. There is a logarithmic relationship between a reaction's activation energy and its rate constant:<sup>15</sup>

$$k = A \cdot e^{-E_a/RT}$$

where  $A$  is the pre-exponential factor ( $M^{-1}s^{-1}$ ),  $E_a$  is the activation energy ( $J/mol$ ),  $R$  is the gas constant ( $J/K \cdot mol$ ), and  $T$  is temperature ( $K$ ). No such relationship has been determined for the strain energy and the rate constant yet. Activation energies are measurable quantities, such as heats of formation. Whereas two species may have very similar strain energies, their heats of formation may vary greatly. The change in heat of formation when travelling from reactant to transition state may not be the same as the change in strain energy. However, it has been determined that strain

energy is thought to reflect the heat of formation, allowing rough correlation between strain energy and kinetics data.<sup>5,16</sup>

As discussed,  $\Delta E_s$  values can be used to estimate the activation energy. High  $\Delta E_s$  values should therefore correlate to low reactivity, and hence small rate constants. Low  $\Delta E_s$  values should correlate to high reactivity, and hence large rate constants. For the series modeled in Figure 15, this correlation is observed. The reaction with the greatest  $\Delta E_s$  (4.77 kcal/mol) correspondingly has the lowest rate constant, 0.01 M<sup>-1</sup>min<sup>-1</sup>. This trend is consistently followed for all reactions modeled; the reaction with the lowest  $\Delta E_s$  (0.14 kcal/mol) correspondingly has the highest rate constant (1200 M<sup>-1</sup>min<sup>-1</sup>). It was therefore reasonably determined that transition state geometries can be modeled on the MAXMIN2 force field using the parameters determined in this study.

The method used to determine the force constants for the Michael addition transition state was similar to that method used for the lactonization. The transition state for the intermolecular nucleophilic attack of water on protonated acrylic acid (Figure 13) was used to simulate the intramolecular Michael addition transition state. Again, this transition state was geometry optimized at the AM1 level. The distances and angles found for this AM1 optimized transition state are used as the equilibrium distance and angle values in the MAXMIN2 force field. The only new distance parameter introduced was for the forming C<sub>1</sub>-O<sub>1</sub> bond. This value was

determined to be 1.75 Å at the AM1 level. The bond stretching constant for the C--O bond was set to 400 kcal/mol·Å<sup>2</sup>. This value is two-thirds the value of MAXMIN2's force constant for an O(sp<sup>3</sup>)-C(sp<sup>2</sup>) bond. Although the bond is not completely formed, there is definite bond character as shown by the energy dependence when this bond length is varied in the AM1 calculations. If this bond is distorted, a relatively significant amount of strain energy should be introduced into the molecule. Therefore, the force constant describing the bond strength should be relatively high. The force constant is not as high as an O(sp<sup>3</sup>)-C(sp<sup>2</sup>), because it was shown that the carbon center under attack has lost a significant amount of its sp<sup>2</sup> character as evidenced by the increased bond length for bond 1 in Figure 13.

An angle parameter was introduced for the attack angle of the nucleophilic oxygen (O<sub>1</sub>-C<sub>1</sub>-C<sub>2</sub> angle), which was determined to be 107.0 degrees at the AM1 level. This value is within the expected range of 100°-110° as suggested by Bürgi and Dunitz<sup>17</sup>, and matches the 107° predicted by Bayly and Grein.<sup>16</sup>

The angle bending force constant was set to 0.02 kcal/mol·deg<sup>2</sup>, only one-fourth of MAXMIN's default parameter for the O(sp<sup>3</sup>)-C(sp<sup>2</sup>)-C(sp<sup>2</sup>) angle type. This low constant was chosen because of the flexibility shown when this angle was varied in the AM1 calculations at a constant bond length. For all other bonds and angles in which the nucleophilic oxygen and the β-carbon are involved, the MAXMIN2 default parameters

for O(sp<sup>3</sup>) and C(sp<sup>2</sup>) were used, respectively. All parameters determined for the MAXMIN2 force field for intramolecular Michael additions are listed in Appendix A, Table 2. Testing of these parameters must be done on series of molecules for which kinetics data is available for comparison. Extensive literature searches are currently being conducted to find such series. This will allow modification of these force constants until a set of parameters is found that gives reliable, predictable results for a number of intramolecular Michael addition reactions.

Currently, the parameters for lactonization and intramolecular Michael addition have been tested on a series of 7 molecules exhibiting competitive reactive sites (scheme 2, where n= 1 to 7) Following a random conformational search on each reactant, the strain energy is calculated using the MAXMIN2 force field. Again, the conformational search is performed to ensure global minima energy conformation for the reactant is being compared to the transition state species. It is vital that the global minimum for each reactant be obtained for comparison. If a local minimum is found and assumed to be the global minimum, the resulting lower energy difference between reactant and transition state may lead to vital errors when reactivity trends are being predicted. Comparison of the energy difference for the two different reactions allows determination of which reaction pathway is kinetically favored for that particular ring size. Table 2

lists the strain energies calculated by the MAXMIN force field for the lactonizations and intramolecular Michael additions of ring size 4 to 10.

ring size	$E_{\text{strain}}$ reactant	$E_{\text{strain}}$ Michael	$\Delta E_{\text{strain}}$	$E_{\text{strain}}$ Lactone	$\Delta E_{\text{strain}}$
4	6.53	115.30	108.8	49.70	43.2
5	2.52	82.96	80.4	8.37	5.9
6	2.25	58.12	55.9	7.04	4.8
7	2.56	56.66	54.1	5.11	2.6
8	2.66	66.60	63.9	12.33	9.7
9	3.09	50.66	47.6	10.43	7.3
10	3.54	55.40	51.9	11.73	8.2

\*All strain energies in kcal/mol

Table 2. Strain energies determined for the reactants, lactonization transition states, and intramolecular Michael addition transition states for the structures A, B, and C in figure 6.

The numerical energy values mean nothing by themselves. Their assignment is merely a technique to quantify the energy increase for a given deviation from an ideal geometry. However, the *differences* in energy between the reactants and transition states can be used to make qualitative predictions about reactivity within a series of closely related structures. It is important to realize that the energy difference *trend*, not the absolute numerical values of the results, is what is important in these studies. The absolute values of the energy differences for the Michael addition series are much greater than for the lactonization series.

This is primarily due to a torsional constraint which had to be used during the optimization of the Michael addition series structured. One of the requirements for the transition state is that the newly forming bond should be co-planar with the enone  $\pi$  system.<sup>16</sup> That is, the torsional angle around the  $\alpha,\beta$ -unsaturated carbon bond (the angle between the planes formed by  $C_1-C_2-C_3$  and  $C_2-C_3-O_1$ ) should ideally be  $90^\circ$ . The reaction involves the LUMO of the conjugated system, a  $\pi^*$  orbital.<sup>13</sup> The nucleophile cannot approach in the nodal plane of the conjugated  $\pi$ -system, and thus it must attack from above or below (Figure 16).

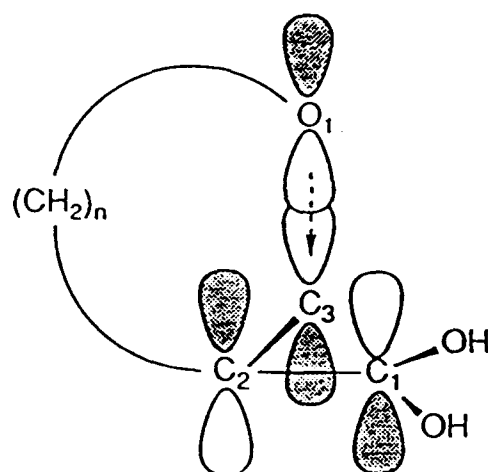


Figure 16. The nucleophilic oxygen must attack from above the nodal plane formed by the conjugated  $\pi$ -enone system. A torsional constraint of  $90^\circ$  was introduced to ensure this stereoelectronic requirement.

This stereoelectronic requirement leads to a large distortion of the normal geometry of the connecting chain of small and medium sized rings and thus introduce strain. A torsional constraint was introduced into the system during the

minimizations to facilitate a realistic angle of attack by the nucleophilic oxygen. This torsional constraint was set to  $90^\circ$  with a force constant of  $200 \text{ kcal/mol} \cdot \text{\AA}^2$ . This force constant was chosen because it did not introduce unrealistic strain into the system, but it did keep this important torsional angle at  $90^\circ$  throughout the minimization procedure. Other constants could be chosen for this constraint and the absolute values of the minimized energy would change for each structure; however, the energy trend for the whole series of Michael additions would remain approximately the same. This illustrates why the magnitude of the strain energies is not as important as the trends they predict.

Before analyzing the results of these calculations, it is wise to have an understanding of the effects of different stereochemical and electronic features on the facility of ring formation. The series of structures modeled was chosen because reactivity trends for similar systems are known. Illuminati and Mandolini have done research on the lactone formation from  $\omega$ -bromoalkane-carboxylate ions (Figure 17).<sup>14</sup> These researchers found trends consistent with previous work on similar systems. The ease of ring formation for the lactonization in Figure 17 is illustrated in Figure 18.

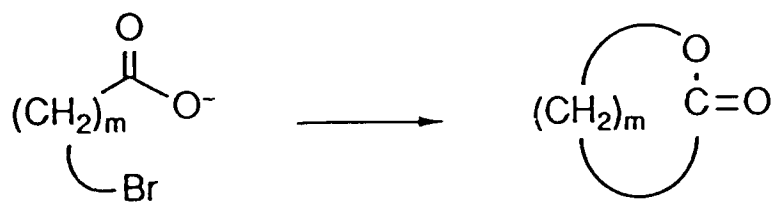


Figure 17.<sup>14</sup> Lactone formation from  $\omega$ -bromoalkane-carboxylate ions.

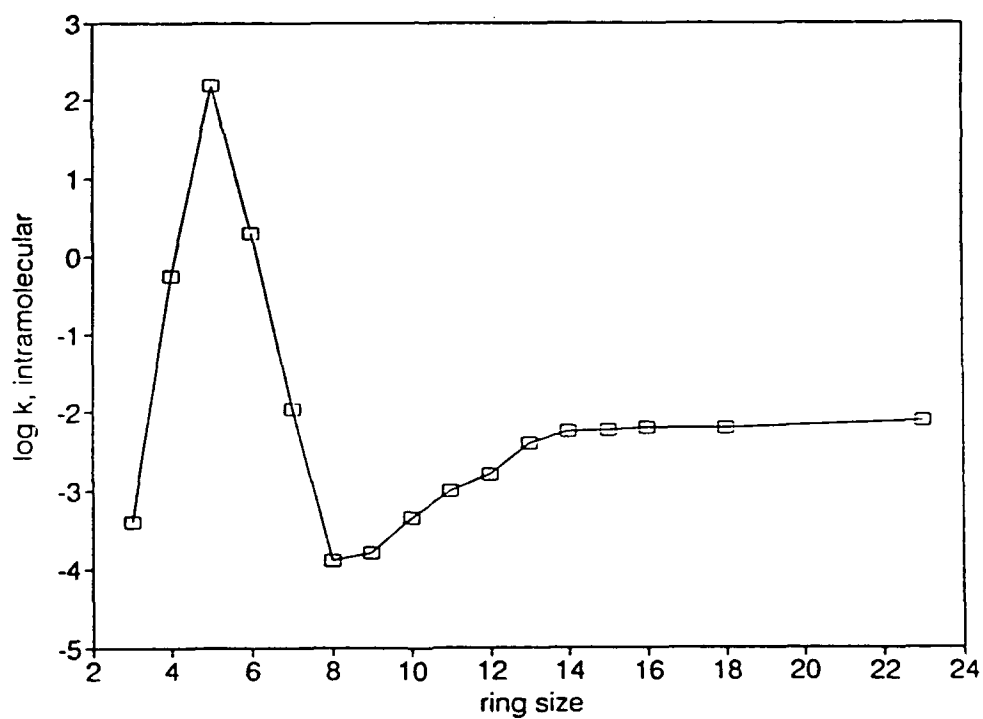


Figure 18.<sup>14</sup> Reactivity profile for lactone formation where  $m=1$  to 21.

These results display some interesting trends:<sup>14</sup>

- On going from the three to the five-membered lactone the rate increases by five powers of ten.

- The rate decreases rapidly to a nadir at the eight-membered ring; the overall decrease is a million-fold.

- For ring size greater than ten, the ease of ring closure increases again until it eventually levels off with the largest rings.

In these and most other ring forming reactions there are two dominant effects which determine the facility of ring formation: ring strain and entropy. For small rings (3- to 4-membered) angle strain and torsional strain are the dominant factors. There are necessarily few conformations possible, making entropy considerations less important. Slightly larger rings (5- to 7-membered) exhibit conformational preferences indicating that cross-ring van der Waals interactions play an important role.<sup>13</sup> Large rings become increasingly flexible and entropy considerations become important.<sup>14</sup>

Analysis of the results of this study predict ring closure facility trends which are acceptable. These trends are shown graphically in Figures 19 and 20, where the difference in strain energy between the bifunctional reactant and the proposed transition state are plotted against the size of ring to be formed. The lactonization reactivity trend provided by this model (Figure 19) is strikingly similar to that determined for Illuminati and Mandolini's similar lactonization system (see Figure 20). The  $\Delta E$ , for the 4-

membered ring is the highest due to the significant strain introduced when orienting the relatively small connecting chain into a cyclic configuration. The rigidity introduced by the  $sp^2$ -hybridized center alpha to the acid causes this  $\Delta E$ , to be a magnitude higher than any of the other lactonizations. The rest of the  $\Delta E$ , values for this series of lactonizations are all relatively low, indicating that their rate constants will all be in the same range of reactivity. All 5-*Exo-Trig* systems, such as this lactonization, are allowed by Baldwin's rules. Therefore, no cutoff  $\Delta E$ , was determined for which this reaction could not occur.

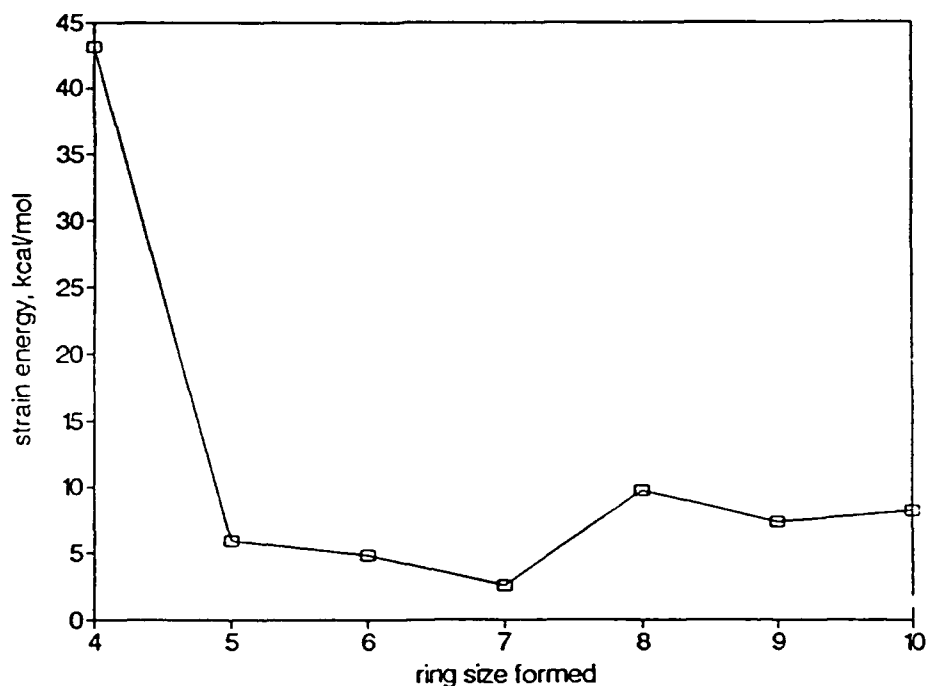


Figure 19. Ring closure facility trend versus ring size formed. The strain energy plotted is the difference in strain energy between the bifunctional chain and the lactone ring.

The ring closure facility trend predicted by this model for the intramolecular Michael addition is shown in Figure 20. According to the model, the highest energy barrier to ring formation is for the 4-membered ring. This is expected because the reactant chain is not long or flexible enough to achieve the ideal transition state structure. The 5-membered ring is slightly lower in energy due to the increased chain length, but steric constraints still cause a high  $\Delta E$ . The energy barrier to formation for the 6 and 7-membered rings is much lower due to the increased number of low energy conformations available with the increased chain length. The increased flexibility in systems this size and larger allow for correct orientation of the atoms involved in the transition state, and thus reaction is more likely to occur. A sudden energy barrier rise is seen for the 8-membered ring. Although the ring is large enough to be relatively free of the strain effects encountered in the 4 and 5-membered rings, trans-annular van der Waals interactions are particularly prominent in 8-membered rings. These interactions are due to electronic repulsion between hydrogens pointing into the interior of the ring. These interactions are inherent in all conformations of 8-membered rings. The 9- and 10-membered rings have relatively small  $\Delta E$  values similar to those of the 5- and 6-membered rings.

This model allows a quantitative interpretation for Baldwin's Rules *Endo-Trig* systems. According to Baldwin's

Rules, 4- and 5-*Endo-Trig* reactions are not allowed, while 6-membered rings and larger are allowed through an *Endo-Trig* intramolecular Michael addition. According to this model, an intramolecular Michael addition with a  $\Delta E$ , less than 63.9 kcal/mol will proceed, while an intramolecular Michael addition with a  $\Delta E$ , greater than 80.4 kcal/mol is not allowed. This  $\Delta E$ , cutoff range for Baldwin's Rule *Endo-Trig* intramolecular Michael additions will be refined when more systems are found in the chemical literature with rate data available for comparison.

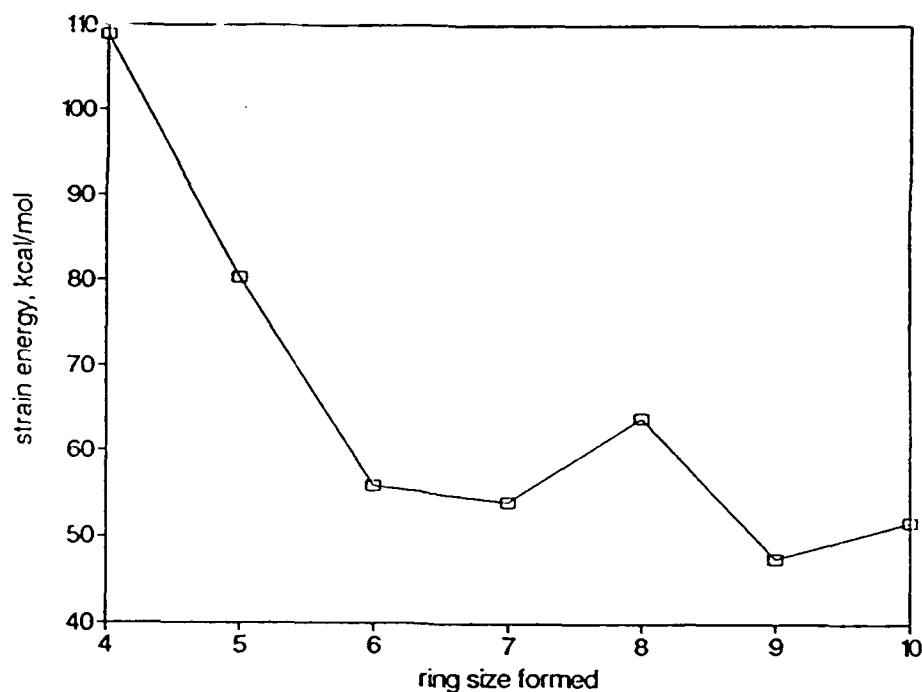


Figure 20. Ring closure facility trend versus ring size formed. The strain energy plotted is the difference in strain energy between the bifunctional chain and the cyclic ether ring formed in the intramolecular Michael addition.

## VII. Conclusions and Further Research.

Models for the prediction of ring closure facility for lactonizations and intramolecular Michael additions were successfully constructed. Based on geometries determined by *ab initio* and semi-empirical calculations for simulated transition states of these reactions, parameters were developed for the MAXMIN2 molecular mechanics force field. Parameters for the lactonization were validated by correctly predicting the reactivity for a series of lactonizations (see Figure 16). Parameters for the intramolecular Michael addition model were proposed and tested on a series of bifunctional reactants.

The trends for ring closure facility through lactonization or intramolecular Michael addition predicted by these models are in relative agreement with models for similar reactions; the trend for lactonization is in close agreement with literature precedents.<sup>14</sup> The trend predicted for intramolecular Michael addition shows similarities to general trends for ring closure reactions.<sup>13</sup> The trend predicted by this model for intramolecular Michael additions may be further refined after additional validation of its parameters is accomplished. This will be done when suitable literature precedents are found with kinetics data; otherwise, experimental work will be done for series of intramolecular Michael additions and kinetics data will be obtained.

## Bond Stretching Parameters

atom types	equilibrium distance	force const
C3-O7	1.292	618.9
C3-O8	1.280	618.9
C3-O9	2.050	309.5
O7-H	0.950	1007.5
O8-H	0.950	1007.5
O9-H	0.950	1007.5

## Angle Bending Parameters

atom types	equilibrium angle	bending const
C2-C3-O7	116.34	0.022
C2-C3-O8	123.22	0.022
C2-C3-O9	116.34	0.022
C3-O7-H	118.37	0.020
C3-O8-H	119.75	0.020
C3-O9-H	123.09	0.010
O7-C3-O8	118.13	0.020
O7-C3-O9	102.17	0.010
O8-C3-O9	97.36	0.010

Appendix A. Table 1. Parameters determined for the simulated lactonization transition state.

## Bond Stretching Parameters

atom types	equilibrium distance	force const
C2-C10	1.335	1340.0
C3-O10	1.430	618.9
C10-O10	1.750	400.0
C10-H	1.089	692.0
O10-H	0.950	1007.5
O5-C2	1.245	1553.0
O5-H	0.999	661.5

## Angle Bending Parameters

atom types	equilibrium angle	bending const
C2-C10-O10	107.0	0.020
C2-O5-H	111.2	0.006

Appendix A. Table 2. Parameters determined for the simulated Michael addition transition state.

Endnotes

- <sup>1</sup>Baldwin, J.E.; Thomas, R.C.; Kruse, L.I.; Silberman, L. J. *Org. Chem.* **1977**, *42*, 3846-52.
- <sup>2</sup>Allinger, N.L. *Adv. Phys. Org. Chem.* **1976**, *13*, 1.
- <sup>3</sup>Hehre, W.J.; Radom, L.; Schleyer, P.v.R.; Pople, J.A. in *Ab Initio Molecular Orbital Theory*, John Wiley and Sons, New York, 1986.
- <sup>4</sup>SYBYL Theory Manual, Tripos Associates, Inc., St. Louis, Mo., 1991.
- <sup>5</sup>Dorigo, A.E.; Houk, K.N. *J. Am. Chem. Soc.* **1987**, *109*, 3698-3708.
- <sup>6</sup>Stewart, J.J.P. *J. Comp.-Aided Design.* **1990**, *4*, 1-105.
- <sup>7</sup>Boyd, D.B.; Lipkowitz, K.B. *J. Chem. Ed.* **1982**, *59*, 269-74.
- <sup>8</sup>Tripos Associates, Inc. is a subsidiary of Evans and Sutherland. SYBYL version 5.4 (1991) was used in this research.
- <sup>9</sup>Allinger, N.L. *J. Am. Chem. Soc.* **1977**, *99*, 8127.
- <sup>10</sup>Powell, M.J.D. *Mathematical Programming*, **1977**, *12*, 241-54.
- <sup>11</sup>Press, W.H.; Flannery, B.P.; Teukolsky, S.A.; Vetterling, W.T. *Numerical Recipes in C, the Art of Scientific Computing*, Cambridge University Press, 1988.
- <sup>12</sup>Saunders, M.; Houk, K.N.; Yun-Dong, W.; Still, W.C.; Lipton, M.; Chang, G.; Guide, W.C. *J. Am. Chem. Soc.* **1990**, *112*, 1419-27.
- <sup>13</sup>Carey, F.A.; Sundberg, R.J. *Advanced Organic Chemistry*, Third Edition, Plenum Press, New York, 1990.
- <sup>14</sup>Illuminati, G.; Mandolini, L. *Accts. of Chem. Res.* **1981**, *14*, 95-102 and references therein.
- <sup>15</sup>Atkins, P.W. *Physical Chemistry*, 4th ed., Freeman, New York, 1990.
- <sup>16</sup>Bayly, C.I.; Grein, F. *Can. J., Chem.* **1989**, *67*, 2173.
- <sup>17</sup>Bürgi, H.-B.; Dunitz, J.D.; Lehn, J.M.; Wipff, G. *Tetrahedron.* **1974**, *30*, 1563-72.

Bibliography of Selected Readings

- Allinger, N.L. *Adv. Phys. Org. Chem.* 1976, 13, 1.
- Allinger, N.L. *J. Am. Chem. Soc.* 1977, 99, 8127-34.
- Allinger, N.L.; Yuh, Y.H.; Lii, J. *J. Am. Chem. Soc.* 1989, 111, 8551-75.
- Atkins, P.W. in *Physical Chemistry*, 4th ed., Freeman, New York, 1990.
- Baldwin, J.E.; Thomas, R.C.; Kruse, L.I.; Silberman, L. *J. Org. Chem.* 1977, 42, 3846-52.
- Bayly, C.I.; Grein, F. *Can. J., Chem.* 1989, 67, 2173.
- Boyd, D.B.; Lipkowitz, K.B. *J. Chem. Ed.* 1982, 59, 269-74 and references therein.
- Broeker, J.L.; Reinhard, W.H.; Houk, K.N. *J. Am. Chem. Soc.* 1991, 113, 5008-17.
- Bürgi, H.-B.; Dunitz, J.D.; Lehn, J.M.; Wipff, G. *Tetrahedron.* 1974, 30, 1563-72.
- Bürgi, H.-B.; Lehn, J.M.; Wipff, G. *J. Am. Chem. Soc.* 1974, 96, 1956-7. Baldwin, J.E. *J.C.S. Chem. Comm.* 1975, 734-741.
- Carey, F.A.; Sundberg, R.J. *Advanced Organic Chemistry*, Third Edition, Plenum Press, New York, 1990.
- Clark, M.; Cramer, R.D.; Van Opdenbosch, N. *J. Comp. Chem.* 1989, 10, 982-1012.
- DeTar, D.F. *J. Am. Chem. Soc.* 1974, 96, 1255-6.
- Dorigo, A.E.; Houk, K.N. in *Advances in Molecular Modeling*, Vol. 1, D. Liotta, ed., JAI Press, Inc., Greenwich, Conn., 1988.
- Dorigo, A.E.; Houk, K.N. *J. Am. Chem. Soc.* 1987, 109, 3698-3708.
- Ellis, G.W.; Tavares, D.F.; Rauk, A. *Can. J. Chem.* 1985, 63, 3510.
- Hehre, W.J.; Radom, L.; Schleyer, P.v.R.; Pople, J.A. in *Ab Initio Molecular Orbital Theory*, John Wiley and Sons, New York, 1986.

- Houk, K.N.; Paddon-Row, M.N. *J. Am. Chem. Soc.* **1986**, *108*, 2659-62.
- Houk, K.N.; Paddon-Row, M.N.; Rondan, N.G.; Yun-Dong, W.; Brown, F.K.; Spellmeyer, D.C.; Metz, J.T.; Li, Y.; Loncharich, R.L. *Science*. **1986**, *231*, 1108-17.
- Illuminati, G.; Mandolini, L. *Accts. of Chem. Res.* **1981**, *14*, 95-102 and references therein.
- Illuminati, G.; Mandolini, L.; Masci, B. *J. Am. Chem. Soc.* **1977**, *99*, 6308-12.
- Mandolini, L. *J. Am. Chem. Soc.* **1978**, *100*, 550-54.
- Powell, M.J.D. *Mathematical Programming*, **1977**, *12*, 241-54.
- Press, W.H.; Flannery, B.P.; Teukolsky, S.A.; Vetterling, W.T. *Numerical Recipes in C, the Art of Scientific Computing*, Cambridge University Press, 1988.
- Rudolf, K.; Hawkins, J.M.; Loncharich, R.J.; Houk, H.N. *J. Org. Chem.* **1988**, *53*, 3879-82.
- Saunders, M. *J. Am. Chem. Soc.* **1987**, *109*, 3150-2.
- Saunders, M.; Houk, K.N.; Yun-Dong, W.; Still, W.C.; Lipton, M.; Chang, G.; Guide, W.C. *J. Am. Chem. Soc.* **1990**, *112*, 1419-27.
- Scheiner, S.; Lipscomb, W.N.; Kleier, D.A. *J. Am. Chem. Soc.* **1976**, *98*, 4770.
- Stewart, J.J.P. *J. Comp.-Aided Design*. **1990**, *4*, 1-105.
- SYBYL Theory Manual*, Tripos Associates, Inc., St. Louis, Mo., 1991.
- Wiberg, K.B.; Martin, E. *J. Am. Chem. Soc.* **1985**, *107*, 5035-41.
- Yun-Dong W.; Tucker, J.A.; Houk, K.N. *J. Am. Chem. Soc.* **1991**, *113*, 5018-27.